Suppression effects in stimulated hyper-Raman emissions and parametric four-wave mixing in sodium vapor

W. R. Garrett, M. A. Moore,* R. C. Hart,† and M. G. Payne
Chemical Physics Section, Oak Ridge National Laboratory, Oak Ridge, Tennessee 37831

Rainer Wunderlich
Division of Geological and Planetary Sciences, California Institute of Technology, Pasadena, California 91125
(Received 11 October 1991)

Experimental investigations of two-photon enhanced stimulated hyper-Raman and parametric four-wave-mixing emissions are described for tuning unfocused laser beams near two-photon resonance with $3D$ and $4D$ states in sodium vapor. Over wide ranges of vapor pressures, path lengths, and laser power densities, the gains for stimulated hyper-Raman (SHR) scattering and for parametric four-wave mixing (PFWM) can become very greatly reduced from values expected from simple considerations. The suppression of gain can arise from interferences produced at two-photon and three-photon resonances, and from ac Stark shifts produced by internally generated near-resonant fields. Quantitative comparisons are made between observed and theoretically predicted values for SHR and PFWM production. Of 12 predicted consequences of the interferences and Stark shifting on the nonlinear behavior, ten are demonstrated through the experiments.

PACS number(s): 42.65.Dr, 32.80.Rm, 42.50.Fx

I. INTRODUCTION

In recent years a number of nonlinear optical studies in a variety of atomic and molecular gases and vapors have established rather unexpected behavior in multiphoton pumping of certain strongly resonant phenomena, where resonant processes that are readily observed under very-low-density (atomic beam) conditions [1] may become almost undetectable at higher densities (though from simple considerations they would be expected to scale with pressure) [2]. These phenomena include (i) the suppression of multiphoton excitation of one-photon allowed transitions by an interference from the sum or difference-mixing field, when such transitions are pumped by an odd number of linearly polarized photons [3–19]; (ii) the suppression of two-photon pumped even-parity transitions where a four-wave-mixing process, either externally driven or internally generated, interferes with direct two-photon laser pumping [20–25]; and (iii) strong suppression of resonant two-photon excitation rates due to broadening and large ac Stark splitting or shifting produced by amplified spontaneous emissions (ASE) and/or stimulated hyper-Raman (SHR) coupling to lower-lying states [25,26]. These suppression mechanisms may manifest themselves as a decrease of laser attenuation by the absorbing medium, reduced production of ASE and SHR emission, and suppressed resonance ionization.

For example, it has been well established that a one-photon allowed atomic transition, when resonantly pumped by an odd number of linearly polarized photons, becomes almost totally suppressed under circumstances where the product of number density N_0 of the resonant species, the oscillator strength F_{0j} for the one-photon transition between states $|0\rangle$ and $|j\rangle$, and the path length z in the medium satisfies the condition $\pi e^2 N_0 F_{0j} z / mc \gg \Gamma$, where Γ is the larger of the laser bandwidth or the pressure-broadened width of the transition (e is the electronic charge, m is the mass of the electron, and c is the velocity of light in the vacuum). The suppression of odd-photon excitation of an optically allowed transition under these conditions results from the influence of an internally generated field arising from sum or difference mixing at the resonant frequency [3]. The internally generated field evolves in such a way that the pumping of the resonant transition by the generated field is equal in magnitude but 180° out of phase with that due to the direct n-photon pumping (odd n). Suppression of such odd-photon mediated multiphoton transitions has been experimentally demonstrated for many cases [4–13] and theoretically described in considerable detail [14–18].

In recent studies [19] we have shown that the odd-photon-resonant interference effect is manifested also in hyper-Raman scattering, wherein stimulated hyper-Raman gain can become suppressed in the forward direction due to the three-photon cancellation effect. The interference effect has yielded predicted and experimentally verified unidirectional backward-propagating stimulated electronic hyper-Raman emission in Na vapor examples [19,25].

In the examples just cited, the suppression effects involve the cancellation of an odd-photon excitation process by interference from a sum or difference frequency mixing field ω_m at the resonant frequency for a one-photon transition between the same two states. Under this circumstance the phase mismatch Δk between a broadband laser field and the sum or difference frequency field is large and complex, and the medium is strongly ab-

 ©1992 The American Physical Society

sorbing at ω_m. However, another form of interference effect can also occur to suppress resonant *two-photon* pumping of an *even-parity* transition. In this second type of interference process involving an even-parity transition, laser-driven two-photon-resonant four-wave mixing [20,22] or internally generated parametric four-wave mixing (PFWM) [20,21] provides an additional pumping mechanism between the ground and two-photon-resonant states.

The interference that cancels resonant two-photon pumping by an internally generated PFWM field occurs under circumstances where the wave mismatch Δk between the laser field and the internally generated fields is zero. Here two separate two-photon Rabi rates, one from direct laser pumping and one from PFWM pumping of the two-photon resonance, become equal in magnitude and opposite in sign. This interference effect was predicted years ago in a detailed steady-state treatment of nonlinear absorption by Manykin and Afanas'ev [20], but was only recently demonstrated experimentally in studies by Malcuit, Gauthier, and Boyd [21], and by Krasnikov, Pshenicknikov, and Solomatin [22]. Malcuit, Gauthier, and Boyd studied suppression of an $s \rightarrow d$ transition in Na by PFWM, and Krasnikov, Pshenicknikov, and Solomatin observed suppression of resonant $s \rightarrow s$ transitions when a second laser, tuned near a one-photon allowed resonance, produced four-wave mixing under conditions where $\Delta k = 0$. The latter process (described as parametric brightening) followed the example predicted in Ref. [20]. The two-photon-resonant interference involving PFWM has been described in a full quantum treatment by Agarwal [23].

In recent studies of parametric processes associated with two-photon excitation of Na $4d$, strong suppressions have been observed of several processes associated with two-photon excitation from the $3s$ onto or near to the $4d$ states of Na [24], leading to decreases in laser attenuation by the absorbing medium [25], reduced ASE from d states, reduced backward hyper-Raman emission associated with lower lying p states, and suppressed resonance ionization associated with pumping of this state. We found that many of the suppression effects could be explained on the basis of the large ac Stark splitting or shifting of the $4d$ state produced by ASE and/or SHR coupling to lower p levels. Other saturation features were readily explained through interference at the two-photon level as produced by phase-matched PFWM production [26]. In the preset study we examine additional details of the suppression mechanisms associated with particular multiphoton processes.

The suppression and/or saturation effects of interest here can occur at laser power densities and vapor pressures where well-recognized saturation phenomena associated with pump attenuation and population transfer processes are still negligible. These processes, which we try to avoid in much of the present study, can add additional saturation characteristics to the phenomena under investigation.

We are thus led to the conclusion that three different suppression mechanisms can apply when an extended resonant medium is pumped near an even- or an odd-photon resonance (in addition to effects due to pump depletion or population transfer). The *three-photon* interference effect can suppress forward SHR emission. ASE and backward SHR emissions can have very high gain in one portion of the resonant medium, but further into the medium ac Stark shifting due to these fields can become very effective in suppressing near-resonant two-photon excitation and greatly reduce gain for stimulated processes. Because of the Stark-based suppression, PFWM, which normally has lower gain, can become comparable to ASE or SHR emissions at high power and/or high number density. Finally, as we discuss below, the nonlinear processes can also exhibit a type of saturation behavior induced by the coherent *two-photon* interference effect mentioned above.

To establish a basis for our subsequent discussion we note some observational facts associated with processes produced by near-resonant two-photon pumping of $s \rightarrow d$ transitions in extended alkali-metal vapors: (i) Pump beam depletion at exact two-photon resonance is much smaller than that predicted on the basis of atomic beam photoionization experiments: thus overall two-photon absorption (from the sum of all processes) is partially suppressed; (ii) stimulated hyper-Raman emission is suppressed in the forward direction, and backward SHR, parametric FWM, and ASE show saturation behavior at high laser power and/or high number density; (iii) the saturation effect mentioned in (ii) has a very sharp onset with pressure at constant laser power, or with laser power at constant pressure; (iv) the backward-propagating SHR profiles show a power- and pressure-dependent dip in line shape at the two-photon resonance; and (v) although at the laser pump intensities used in these experiments SHR emission has higher gain than PFWM, nevertheless PFWM emissions can be comparable to SHR intensities. All of the effects can be operative in regimes where laser beam attenuation and population transfer are not significant. Indeed, we will show that the processes to be considered below cause population transfer to become greatly reduced from expected magnitudes.

We have conducted a series of experiments and corresponding theoretical calculations [27] for processes associated with $s \rightarrow d$ two-photon pumping and $s \rightarrow p$ three-photon pumping (through SHR scattering) in Na vapor. In these studies we delineate the respective roles of ac Stark effects and PFWM interferences in suppressing results from values normally expected for two-photon resonantly enhanced phenomena, and we explain quantitatively the five features listed above. The three separate mechanisms that lead to gain suppression in the processes of interest here were mentioned above. The consequences of SHR gain suppression by odd-photon interferences (three- and five-photon cases) are described in Sec. III. Results due to limitation of SHR gain by ac Stark shifting are the subjects of Sec. IV. Finally, consequences of limitations on the gain for PFWM from interference at the two-photon level are described in Sec. V. The choice of ordering is based on the fact that the effects in Sec. II and in Sec. IV mainly influence SHR emissions, while that in Sec. V influences PFWM production.

II. EXPERIMENTAL ELEMENTS

The apparatuses used in the various experiments included a stainless-steel heat pipe oven to generate and contain Na vapor at pressures up to a maximum of ≈ 8 Torr. The heat pipe contained an internal thermocouple and charge-collecting wire, which traversed the entire vapor region. The device was operated with argon buffer gas. Both an excimer pumped dye laser system (Lumonics 861T and EDP 330) and a Nd:YAG (neodymium-doped yttrium aluminum garnet) pumped dye laser system (Lumonics HD 300) were used in the experiments. The excimer system delivered 4–5 ns pulses with maximum energy of 1.5 mJ/pulse near 685.5 nm ($3s$-$3d$ pumping) and 8 mJ/pulse near 578.8 nm ($3s$-$4d$ pumping). Beam diameter was 3.0 mm, and maximum unfocused power densities were 5×10^6 and 2.8×10^7 W/cm^2, respectively. Laser bandwidth was ≈ 0.04 cm^{-1}. The Nd:YAG system delivered power densities up to 60 MW/cm^2 at a bandwidth similar to the excimer-based system. Na emissions were variously recorded with a Jarrell Ashe spectrometer of 0.03 nm resolution and/or filtered photodiodes. Laser energies and energies of stimulated emission processes were measured with a Scientech 362 power meter or in certain instances with calibrated photodiodes.

III. SUPPRESSION OF FORWARD COMPONENTS OF STIMULATED HYPER-RAMAN EMISSION BY FWM INTERFERENCE

As mentioned in the Introduction, the nonlinear optical effect associated with odd-photon pumping of transitions that are one-photon allowed is a well-studied phenomenon [2–18]. When such transitions are pumped by unidirectional laser beams, an electric polarization is generated in the medium at the frequency of the one-photon resonance (the sum or difference frequency of the pumping fields). Under well-described circumstances, the field produced by this polarization can grow to a value such that the resultant pumping of the atomic transition from this internally generated source is equal in magnitude but opposite in phase to that from odd-photon pumping by the externally applied laser fields. At this point the two pumping mechanisms cancel each other. No further excitations occur. The polarization likewise saturates and undergoes no additional increase in magnitude as the beams propagate further through the medium. If oppositely directed beams are used for the odd-photon excitation, the n-wave mixing field is still generated, but the suppression effect is drastically different. With the use of counterpropagating beams the excitation process occurs as expected but with a pressure-dependent shift, as recently demonstrated in studies in Xe [28]. Even if independent uncorrelated lasers of different frequencies are used to drive the odd-photon excitation, the interference prevents excitation, unless the beams are propagated at crossing angles exceeding a critical value [28]. Unlike most nonlinear processes, the cancellation effect is independent of intensities of any of the pump lasers. These aspects have been demonstrated by Garrett, Henderson, and Payne [8] for three-photon excitation in Xe. The interference effect has also been shown to occur for five-photon pumping under conditions where an interference is produced by six-wave mixing [9].

A. Prediction of forward stimulated hyper-Raman gain suppression

Now consider the stimulated hyper-Raman (SHR) process, and a simplified three-state atomic mode for its description (Fig. 1). Two laser photons at angular frequencies ω_1 and ω_2 are near two-photon resonance between states $|0\rangle$ and $|2\rangle$ (detuning δ_2) to produce a two-photon Rabi frequency $\Omega^{(2)}_{0,2}$. (In the present context, where one laser is used, $\omega_1=\omega_2\equiv\omega_L$.) Weak fields generated at the hyper-Raman frequency $\omega_{\rm HR}$ couple to state $|3\rangle$ at $\omega_{\rm HR}=2\omega_L-E_3/\hbar$, where E_3 is the energy of level $|3\rangle$. Note that the SHR process does not involve the two-photon resonance *per se,* but is greatly enhanced by the increase in the magnitude of $\Omega^{(2)}$ that results from tuning near a two-photon resonance. If the initial spontaneous start-up is neglected, the SHR process can be described through a polarization source term that arises from the atomic response at $\omega_{\rm HR}$. However, we must be careful to note that an important direction asymmetry exists in the nonlinear field generated parallel and antiparallel to the pump-laser beam. In the forward (parallel) direction the combination of laser and hyper-Raman fields together creates a traveling-wave polarization at the

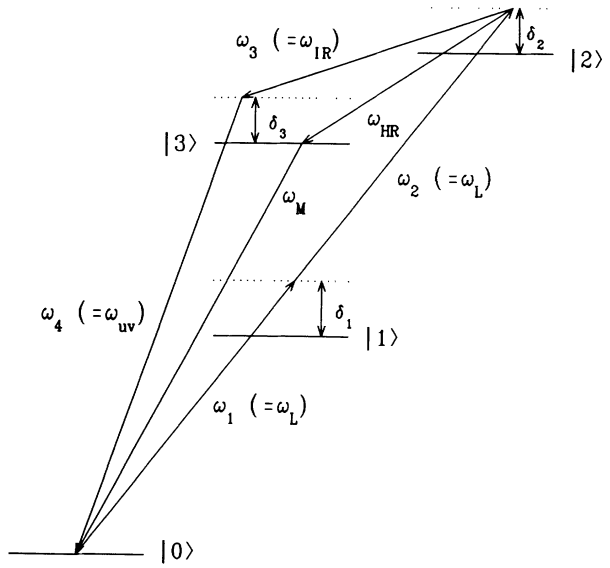

FIG. 1. Simplified level scheme for the present treatment of SHR emission and PFWM production. Level $|1\rangle$ is adiabatically eliminated, thereby reducing the problem to a three-level model. The SHR process leads to excitation of $|3\rangle$ accompanied by stimulated emission at $\omega_{\rm HR}$. The SHR field and the laser field together generate a coherent four-wave difference-mixing field ω_M. The field at ω_M is strongly absorbed. In the PFWM process frequencies $\omega_{\rm IR}$ and $\omega_{\rm UV}$ are generated such that $2\omega_L=\omega_{\rm UV}-\omega_{\rm IR}$ and $\Delta k=0$. Also defined are δ_1, δ_2, and δ_3, which are detunings from exact resonance with the respective levels.

four-wave difference-mixing frequency $\omega_m = 2\omega_L - \omega_{HR}$. This is also the resonant frequency for a $|0\rangle \rightarrow |3\rangle$ transition. Moreover, from previous work [3,7,8,14] we know immediately that the four-wave-mixing field ω_m will evolve such that the one-photon Rabi rate connecting $|0\rangle$ and $|3\rangle$ through ω_m is equal in magnitude and 180° out of phase with the three-photon pumping by $2\omega_L - \omega_{HR}$. Thus the two mechanisms connecting states $|0\rangle$ and $|3\rangle$ will interfere in the forward SHR emission process to suppress the gain for forward SHR generation. The backward SHR production should show normal gain. (It will exhibit a pressure-dependent redshift [28–30], which is too small to be observed at the number densities available in the present context.) Note that the interference will occur only with SHR emission associated with excitation of a state that is dipole coupled to the ground state (i.e., $\langle 3|\hat{D}|0\rangle \neq 0$, where $\hat{D}$ is the electric dipole operator). Of course some SHR processes will not show the interference in forward emission since the dipole coupling condition between $|0\rangle$ and $|3\rangle$ need not be satisfied in all cases.

A fairly concise proof of the cancellation effect involving SHR emission can be given by breaking the SHR generation into forward and backward components, and showing that the forward component is accompanied by a four-wave difference-frequency mixing field that can be put into a form that has already been shown in earlier studies to produce destructive interference in the electronic excitation associated with the SHR scattering [3,18,27]. An experimental demonstration of the effect has been published earlier by the present authors [19].

We describe the atomic response through a three-state model where the time-dependent wave function for an atom at z is

$$|\Psi(z,t)\rangle = e^{-i\omega_0 t}[a_0(z,t)|0\rangle + a_2(z,t)e^{2i(k_L z - \omega_L t - \theta_L)}|2\rangle + a_3(z,t)e^{2i(k_L z - \omega_L t - \theta_L)}e^{i\omega_{HR} t}|3\rangle] . \tag{1}$$

The states $|i\rangle$ are eigenstates of the Hamiltonian for isolated atoms with eigenvalues $\hbar\omega_i$. We use a phase convention that removes rapidly oscillatory phase factors from the equations for the amplitudes $a_i(z,t)$. Equations of motion are derived for an atom subjected to a plane-wave laser field E_L, tuned near two-photon resonance between states $|0\rangle$ and $|2\rangle$, and to laserlike internally generated fields E_{HR} and E_M. The hyper-Raman field E_{HR} has forward-directed component E^+_{HR} (parallel to the laser field) and backward component E^-_{HR}. Two photons from the laser beam combined with a hyper-Raman photon provide resonant three-photon pumping of state $|3\rangle$. A polarization of the medium at frequency $\omega_m = 2\omega_L - \omega_{HR}$ is also created by these fields. This polarization has an associated four-wave-mixing field E_M at ω_m. These fields are defined respectively as

$$E_L = E_{L0}(t - z/v_L)\cos[\omega_L t - k_L z + \theta_L(t - z/v_L)] , \tag{2a}$$

$$E_{HR} = E^+_{HR} + E^-_{HR} , \tag{2b}$$

$$E^{\pm}_{HR} = \frac{E^{\pm}_{HR0}}{2}\exp[i(\omega_{HR} t \mp k_{HR} z)] + \text{c.c.} , \tag{2c}$$

$$E_M = \tfrac{1}{2}E_{M0}e^{i\omega_M t} + \text{c.c.} \tag{2d}$$

The laser field has phase velocity v_L, and propagation vector $\mathbf{k}_L$. The amplitude E_{L0} and phase θ_L of the laser field (and the other fields) are assumed to vary slowly with respect to $\cos(\omega_L t - k_L z)$. For broad-bandwidth lasers the amplitudes and the phases are assumed to undergo fluctuations during a pulse, with durations of the order of magnitude of the inverse laser bandwidth. Couplings between the three relevant states, as depicted in Fig. 1, are written in terms of reduced Rabi frequencies $\Omega_{n,m}(z,t) = D_{n,m}E/2\hbar$, where $D_{n,m}$ is a matrix element of the electric dipole operator $\hat{D}$ between states n and m. Moreover, state $|1\rangle$ can be adiabatically eliminated to produce a reduced two-photon Rabi frequency $\Omega^{(2)}_{0,2}$, thereby reducing the problem to a three-state model.

The reduced Rabi frequencies are defined as

$$\Omega_{3,0}(z,t) = \frac{D_{3,0}E^*_{M0}}{2\hbar} , \tag{3a}$$

$$\Omega^+_{2,3}(z,t) = \frac{D_{2,3}E^+_{HR0}}{2\hbar} , \tag{3b}$$

$$\Omega^-_{2,3}(z,t) = \frac{D_{2,3}E^-_{HR0}}{2\hbar} , \tag{3c}$$

$$\Omega^{(2)}_{0,2}(z,t) \simeq \Omega_{0,1}\Omega_{1,2}/\delta_1 , \tag{3d}$$

where $\Omega_{0,1}$ and $\Omega_{1,2}$ are the reduced Rabi frequencies for coupling by the laser field of states $|0\rangle$ and $|1\rangle$ and $|1\rangle$ and $|2\rangle$, respectively.

With these fields, equations of motion for the amplitudes $a_i(z,t)$ are obtained in standard fashion [24],

$$\frac{\partial a_0}{\partial t} = i\Omega^{(2)}_{0,2}a_2 + i\Omega_{0,3}e^{2i(k_L z - \theta_L)}a_3 , \tag{4a}$$

$$\frac{\partial a_2}{\partial t} = i\left[\delta_2 + 2\frac{\partial \theta_L}{\partial t}\right]a_2 + i\Omega^{(2)}_{2,0}a_0 + i(\Omega^+_{2,3}e^{ik_{HR}z} + \Omega^-_{2,3}e^{-ik_{HR}z})a_3 , \tag{4b}$$

$$\frac{\partial a_3}{\partial t} = i\left[2\frac{\partial \theta_L}{\partial t} + i\gamma_3/2\right]a_3 + i\Omega_{3,0}e^{-2i(k_L z - \theta_L)}a_0 + i(\Omega^+_{3,2}e^{-ik_{HR}z} + \Omega^-_{3,2}e^{ik_{HR}z})a_2 . \tag{4c}$$

Here $\delta_2 = 2\omega_L - (\omega_2 - \omega_0)$, $\hbar\omega_0$ is the energy of the ground state, $\hbar\omega_2$ is the energy of the two-photon state $|2\rangle$, and γ_3, the total spontaneous decay rate, is included to simulate the natural width of the line. We suppress z and t arguments of a_i and $\Omega_{i,j}$.

The electric polarization of the medium $P = N\langle\Psi(z,t)|\hat{D}|\Psi(z,t)\rangle$ provides source terms for the generated fields. (Here N is the number density.) The suppression effect can be most readily revealed by considering the polarization $P_M(\omega_m) \equiv P_M(2\omega_L - \omega_{HR})$, which serves as a source term for the generation of the four-wave difference-mixing field E_M. We divide this polarization into a resonant and a nonresonant part [14,27], P^R_M

and $P_M^{\rm NR}$, respectively,

$$P_M = P_M^R + P_M^{\rm NR} . \tag{5a}$$

The term $P_M^{\rm NR}$ is the linear polarization term due to all off-resonant levels that are dipole coupled to the ground state. P_M^R is the resonant contribution to this polarization, which contains a linear component in E_M and a nonlinear component that is quadratic in the laser field and linear in the hyper-Raman field. The resonant part of P_M is [24]

$$P_M^R = ND_{0,3} a_0^* a_3 e^{2i(k_L z-\theta_L)} e^{-i(2\omega_L-\omega_{\rm HR})t} + \text{c.c.}$$
$$= ND_{0,3} Y(z,t) + \text{c.c.} \tag{5b}$$

For convenience the polarization component $P_M^R(\omega_m)$ is expressed in terms of a reduced polarization $Y(z,t)$ such that $P_M^R = ND_{0,3}Y(z,t) + \text{c.c.}$, or

$$Y(z,t) = a_0^* a_3 e^{2i(k_L z-\theta_L)} e^{-i(2\omega_L-\omega_{\rm HR})z/v} . \tag{5c}$$

The polarization $P_M(\omega_m)$ is the source term in Maxwell's equation for the four-wave-mixing field E_M. The field E_M satisfies

$$\frac{\partial^2 E_M}{\partial z^2} - \frac{1}{v^2}\frac{\partial^2 E_M}{\partial t^2} = \frac{4\pi}{c^2}\frac{\partial^2 P_M^R}{\partial t^2} .$$

We consider only unfocused beams treated in a plane-wave approximation. Maxwell's equation, for no incoming wave, is solved in terms of an integral of $\partial P_M^R/\partial t$ over the length of the nonlinear medium. The solution has the form [14]

$$E_M = -\frac{2v\pi}{c^2}\int_0^L dz' \frac{\partial P_M^R(z', t-|z-z'|/v)}{\partial t} . \tag{5d}$$

The procedure utilized earlier by Payne and Garrett [14] to obtain Maxwell-Bloch equations for the reduced polarization Y is again followed. The equation for E_M is substituted back into the equation of motion for the bilinear product $a_0^* a_3$ (or the equation for Y). We note that in evaluation of the integral in Eq. (5d), the major component of the partial derivative of the polarization comes from the complex exponential factor, and in the integral over z' the interval from z to L can be neglected. Thus if we evaluate E_M from Eq. (5d) and make use of the definition (4a) for the Rabi frequency $\Omega_{3,0}$ that involves E_M, we can arrive at

$$\Omega_{3,0}(z,t) \simeq i\kappa_{0,3} e^{i(2\omega_L-\omega_{\rm HR})z/v} \int_0^z dz' Y(z', t-(z-z')/v) , \tag{5e}$$

where

$$\kappa_{0,3} = \frac{2\pi N|D_{0,3}|^2(2\omega_L-\omega_{\rm HR})}{\hbar c} . \tag{6}$$

Finally we restrict present consideration to circumstances where ground-state depletion is negligible, $a_0 \simeq 1$, and from Eq. (4b), $a_2 \simeq -\Omega_{2,0}^{(2)}/\delta_2$. With these approximations for a_0 and a_2 and with the use of Eq. (3c) for a_3, we obtain a coupled Bloch-Maxwell equation for the reduced polarization $Y(z,t)$ in the form

$$\frac{\partial Y(z,t)}{\partial t} = -\kappa_{0,3}\int_0^z dz' Y(z', t-(z-z')/v)$$
$$+ i(\delta_3 + i\gamma_3/2) Y(z,t)$$
$$- i\frac{\Omega_{2,0}^{(2)}}{\delta_2} e^{i(\mu z - 2\theta_L)} (\Omega_{3,2}^+ + \Omega_{3,2}^- e^{2ik_{\rm HR} z}) , \tag{7}$$

where

$$\mu = [2k_L - k_{\rm HR} - (2\omega_L - \omega_{\rm HR})/v] ,$$
$$\Omega_{3,2}^+ = D_{3,2} E_{\rm HR0}^+ / 2\hbar ,$$

and

$$\Omega_{3,2}^- = D_{3,2} E_{\rm HR0}^- / 2\hbar .$$

In Eq. (7), $\Omega_{3,2}^+$ is the Rabi frequency between states $|2\rangle$ and $|3\rangle$ due to the forward-directed hyper-Raman beam, and $\Omega_{3,2}^-$ is that due to the backward-directed emission. The polarization can thus be further broken down into components involving forward- and backward-propagating fields. Thus if $Y(z,t)$ is written as

$$Y(z,t) = Y^+(z,t) + Y^-(z,t) , \tag{8a}$$

where Y^+ is associated with Ω^+ and Y^- is associated with Ω^- in Eq. (7), we can obtain an equation for Y^- and Y^+. If this decomposed form of Y is substituted into Eq. (7), the integral term having Y^- as the integrand has a very rapid oscillatory dependence on z that allows an asymptotic evaluation of $\int_0^z dz' Y^-(z', t-(z-z')/v)$. This term produces a pressure-dependent shift in the position of the resonant gain for the backward SHR [28], which is too small to be observed in the context of the present heat pipe studies. We completely neglect the integral over Y^-, which allows the resulting equation for Y^- to be solved with the result

$$Y^-(z,t) = -\frac{i}{\delta_2} e^{i(\mu+2k_{\rm HR})z} \int_{-\infty}^t dt' e^{is(t-t')} e^{-2i\theta_L}$$
$$\times \Omega_{2,0}^{(2)}(z,t') \Omega_{3,2}^-(z,t') , \tag{8b}$$

where $s = \delta_3 + \kappa_{0,3}/(2k_{\rm HR}) + i\gamma_3/2$.

Again from Eq. (7), after neglecting the integral over Y^-, we see that the component $Y^+(z,t)$ of the reduced polarization, propagating in the $+z$ direction, satisfies the inhomogeneous integro-differential equation

$$\frac{\partial Y^+(z,t)}{\partial t} \simeq -\kappa_{0,3}\int_0^z dz' Y^+(z', t-(z-z')/v)$$
$$+ i(\delta_3 + i\gamma_3/2) Y^+(z,t)$$
$$- i\frac{\Omega_{2,0}^{(2)}}{\delta_2} \Omega_{3,2}^+ e^{i(\mu z - 2\theta_L)} . \tag{8c}$$

We now make five points about the form of Eqs. (8b) and (8c), which describe the backward and forward components of the electric polarization at ω_M. First, note that Eq. (8c), describing the reduced polarization resulting from pumping by two laser photons and one *forward* SHR photon, has been put into exactly the same form as that studied extensively by Payne, Garrett, and coworkers [3,14,18], where the pumping was affected by

three laser photons. Second, it was found in these previous studies that under circumstances where the product of number density N and $|D_{0,3}|^2$ is such that $\kappa_{0,3}$ is large ($\kappa_{0,3} \propto N|D_{0,3}|^2$) and strong resonant absorption of ω_M occurs, the partial derivative on the left of Eq. (8c) becomes very small as compared to either of the other terms. In this limit the last two terms on the right-hand side are equal in magnitude and of opposite sign. This condition produces a cancellation of the corresponding pumping of $|3\rangle$ by the combination of the FWM field E_M and the three-photon pumping involving the absorption of two laser photons and the stimulated emission of a forward hyper-Raman photon. The solution for Y^+ in this limit is very small; thus for all z along the laser path, the atomic response is such that $Y^+ \simeq 0$ and thus $a_3 \simeq 0$. This means also that $\partial a_3/\partial z \simeq 0$. Third, the interference that suppresses the magnitude of the polarization at ω_m is independent of the magnitudes of E_L and E_{HR}; thus it develops as the fields grow up from the noise.

The result from Eq. (8c) is that pumping of $|3\rangle$ by the lased field and forward stimulated hyper-Raman scattering when combined with pumping by the generated FWM field yields $Y^+ \sim 0$. Thus no stimulated excitation of $|3\rangle$ is produced by the copropagating laser and SHR fields. The cancellation becomes pronounced when $\kappa_{0,3}\Delta z/\Gamma \gg 1$ where Δz is a small fraction of the length of the laser path through the medium and Γ is the larger of the laser bandwidth and Doppler width of the line for the transition between $|0\rangle$ and $|3\rangle$. Fourth, the generation of the SHR field can be written in terms of a source term, the SHR polarization $P_{\mathrm{HR}} = ND_{2,3}a_2^* a_3 e^{i\omega_{\mathrm{HR}}t}$ +c.c., and since this forward SHR polarization is proportional to the corresponding component of $a_2^* a_3$, it also remains small. Thus the forward SHR gain is effectively reduced to zero after building up to only a tiny fraction of its expected value. Fifth, because of the great difference in phase considerations, the interfering FWM field associated with the backward SHR will only produce an unobservable shift [28] in ω_{HR}; otherwise, the SHR emission in the backward direction should be normal, with high gain in our example [27].

One further note concerning the interference effect is germane to studies in alkali-metal vapors. It is obvious that excitation of an nF_J state by SHR scattering would not involve an interference in the forward gain, since $\langle 3|\hat{D}|0\rangle = 0$ in such a case. However, not as obvious is another possibility of this type involving $S \rightarrow P$-state excitation. If circularly polarized light is used to pump the SHR process, then a $|\Delta m| = 2$ excitation can be mediated through SHR emission if the HR scattering involves $\Delta m = 0$ (linearly polarized ω_{HR}). Thus, starting with $m = \mp 1/2$ an $nP_{3/2}$ state can be excited with $m = \pm 3/2$, for right- or left-circular polarization of the pump, respectively. Then $\langle 3|\hat{D}|0\rangle$ is zero, and no interference will occur for this case. This same process cannot excite a $P_{1/2}$ level. Thus with circularly polarized light it should be possible to produce forward SHR connecting a $P_{3/2}$ but not a $P_{1/2}$ level. We return to this point below.

Finally we note that a more approximate treatment of the hyper-Raman suppression effect has also been presented by Malakyan [31], though the system of equations was not shown to evolve to satisfy the condition for interference [14,20], only that this is a possible consequence of the atomic response.

B. Experimental studies in Na vapor

We previously reported on a set of experiments designed to demonstrate forward gain suppression in hyper-Raman emission [19]. In that study, ground-state sodium atoms were pumped with linearly polarized light near two-photon resonant $3d\,^2D_{3/2,5/2}$ and $4d\,^2D_{3/2,5/2}$ states to produce resonantly enhanced SHR emissions associated with excitation of lower-lying P states (both $P_{1/2}$ and $P_{3/2}$ components). The driven wave at the resonant frequency connecting either of the $3p$ or $4p$ states to the $3s$ ground state was the fourth wave in the FWM process mentioned above. (See Fig. 1.) We predict, e.g., that the two SHR emissions that result from pumping near the two-photon-resonant $3d$ state to excite $3p_{1/2}$ and $3p_{3/2}$ states will both occur only in the direction opposite that of the laser beam (where the emissions are near 819 nm). Likewise, the SHR associated with tuning near two-photon resonance with Na $4d$ should show the same effect at the two emissions near 569 nm, associated with $3p_{1/2}$ and $3p_{3/2}$ states, and two near 2.3 μm, associated with $4p_{1/2}$ and $4p_{3/2}$ excitations.

When the incident laser is tuned *exactly* to two-photon resonance $\delta_2 = 0$, the $d \rightarrow p$ emission process changes character, since energy can then be stored in the d states, and amplified spontaneous emission replaces the SHR mechanism. The ASE photons incoherently excite $|3\rangle$ through a process that can be time delayed with respect to the laser field. Such emission involves no interference effect, and thus it has gain in the forward or backward direction.

Finally, we note that, in addition to the SHR process, parametric FWM may also occur under the conditions being considered. This process produces photons at ω_3 and ω_4 where ω_3 is near but not equal to, ω_{HR} and ω_4 is near $(E_3 - E_0)/\hbar$. Due to phase-matching considerations, this FWM light is emitted only in the forward direction, usually over a distribution of angles in a cone about the laser beam. The process has been well documented for Na by Krasinski *et al.* [32]. The ASE or SHR emissions can be distinguished from the parametric FWM by spectral and/or polarization differences or, in some instances, by the physical separation between conical and axial propagation, or by directionality.

In the present instance the unfocused linearly polarized laser beam was apertured to a 3-mm diameter before entering the heat pipe to produce a near-Gaussian beam profile. Special care was taken to insure that collection techniques for both forward and backward beams were matches so as not to produce preferential detection of either beam. Both were collected by glass wedges that reflected $\sim 4\%$ per surface reflection. (See Fig. 2.) Guiding of the respective beams into the spectrometer was accomplished by rotating a 99% reflecting aluminum mirror to project one or the other of the beams onto the en-

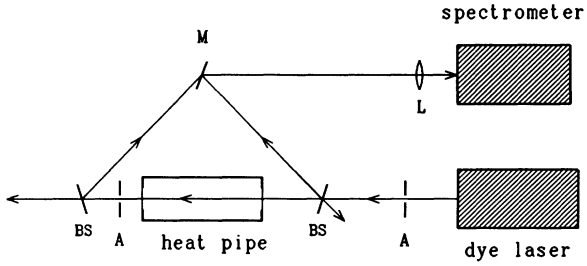

FIG. 2. Experimental arrangement for measurements of backward and forward emissions from a sodium-vapor heat pipe. Elements A are apertures, BS are wedged beam splitters, and M is a rotatable aluminum-coated mirror.

trance slit. The path length between heat pipe center and spectrometer differed at maximum by only 4 cm. Spectrometer scans of SHR emissions were alternated between forward and backward directions, keeping the laser frequency fixed, to assure that both beams were compared at exactly the same laser frequency [19].

Shown in Fig. 3 are spectrometer scans of backward (upper trace) and forward (lower trace) emissions in the 820-nm region obtained when tuned onto the Na $3D$ resonance ($\delta_2=0.0$). The data are for sodium pressure of 1.9 Torr and laser intensity of 2.0×10^7 W/cm^2. The backward emission in the upper trace is ASE associated with emission from the $3D_{3/2}$ and $3D_{5/2}$ to the $3P_{1/2}$ and $3P_{3/2}$ levels. The lower trace shows both forward ASE and PFWM emission since both are produced in this direction. At a sodium vapor pressure of 1.9 Torr some of the conical FWM is produced at angles too large to be focused onto the entrance slit of the spectrometer. (This is unimportant here.)

In Fig. 4 we show corresponding traces of backward and forward emissions obtained under off-resonant pumping, $\delta_2=0.05$ nm. This detuning is larger than the laser bandwidth; thus there is no overlap with the $3D$ levels and the backward emission in the upper trace is pure SHR instead of ASE. The forward emissions now show three emission profiles, none of which occurs at the SHR frequencies. Indeed, in the forward direction there are no detectable signals at either of the SHR wavelengths. We note in passing that the three PFWM profiles on the lower trace of Fig. 4 are all produced by light collected at fairly low angles ($\leq 3°$). If collection is limited to include only strictly axial emissions, the broad peak on the left is excluded. The other two remain. The center profile is associated with axial PFWM, as discussed in some detail elsewhere [33]. The profile at longer wavelength, on the right, only appears at high pump intensities and Na density above 1 Torr, where population transfer to the $3P$ levels can cause the medium to be dispersive at ω_3 as well as at ω_4, thus allowing additional axial FWM production over the late part of a laser pulse. We have intentionally chosen to show data where axial emission does occur in the forward direction. However, it is obvious from the spectral content that the source of this forward-directed light is not SHR, in agreement with our previous prediction.

In Fig. 3 we note that the ASE peaks in the backward direction are considerably larger than the corresponding forward components, though this emission would be expected to have similar gain along either axial direction. This can be readily explained, and by pumping at lower laser intensity where the axial PFWM gain becomes very low, the suppression of forward SHR emission can be demonstrated in another way, as follows.

We introduce a 5-mm aperture in the forward beam to discriminate against the conical emission associated with forward-directed, angle phase-matched PFWM. This provides good spatial separation of any laserlike axial beam from the conical PFWM process (see Fig. 2.) Displayed in Fig. 5 are results showing forward and backward apertured emissions, near 819.7 and 818.5 nm, obtained from tuning near the $3d$ states with $\sim10^6$ W/cm^2 of laser intensity.

The upper pair of traces in Fig. 5 show forward and backward components at zero detuning from the $3D$ state. Again, as in Fig. 3, notice that forward ASE intensity is smaller than that of the backward component, though the emission is almost all bidirectional ASE. However, since the bandwidths of our laser exceeds the Doppler broadened atomic linewidth, some SHR emission is also produced at "exact" resonance. That is, that portion of the laser frequency profile that does not overlap the narrow atomic excitation profile only produces hyper-Raman scattering, but it only has gain in the counterpropagating direction. Hence the backward beam is more intense even at $\delta_2=0$. Note that the small peak in the top trace of Fig. 5, which appears between the two ASE emissions, is due to the axially phase-matched parametric four-wave-mixing process [33] not associated with any population transfer. All conical PFWM is effectively blocked by the aperture.

In the middle pair of traces in Fig. 5 the laser is detuned to the high-energy side of the $3d$ resonance by 0.01 nm. The intensity of the forward beam drops drastically while the backward beam is affected only minimally. At 0.03 nm detuning to the high-energy side of the resonance [lower pair of traces in Fig. 5] the emission in the forward direction is almost totally suppressed, as predicted, while the backward SHR, although weaker, is still easily observable. In this instance (28 cm vapor column length) the suppression should be effective at Na pressures above $\sim10^{-4}$ Torr.

Finally, we also recognize the obvious fact that the absence of any SHR component in forward emissions and the absence of any PFWM component in the backward emissions means that the excitation profiles for production of forward and backward light will look quite different whether one observes all of its spectrally or specially resolved fractions. We show one example of this part of the behavior in Fig. 6. These traces show total output of forward and backward emission as a function of pump-laser wavelength. As expected, the excitation profiles have practically nothing in common.

Now consider PFWM when two-photon pumping near Na $4d$. The susceptibility for the parametric process is

resonantly enhanced for photons generated in near resonance with the $4p_{3/2}$ and the $4p_{1/2}$ states, where the generated photons are approximately 2.3 μm and 330.3 nm. But the oscillator strengths between the $4p$ levels and the $3s$ ground state are small (0.0094 and 0.0047 for the $4p_{3/2}$ and $4p_{1/2}$, respectively). The Na vapor is fairly negatively dispersive for the laser photons of $\sim$579 nm, since this photon energy is only $\sim$300 cm^{-1} above the $3p$ sublevels, both of which have large oscillator strengths to the ground state. Since the medium is only weakly dispersive for each of the $\sim$330-nm components of the PFWM process, phase matching can occur in four narrow-frequency regions for the UV (and corresponding IR) photons, where the UV frequencies in every case are very near the $4p_{3/2} \rightarrow 3s_{1/2}$ or $4p_{1/2} \rightarrow 3s_{1/2}$ resonant frequencies. That is, the usual angle phase-matched PFWM occurs at frequencies that are positively dispersive for the UV; one process occurs in a UV energy region slightly below the $4p_{3/2}$ level and another occurs in a region just below $4p_{1/2}$, where phase matching is achieved through the generation of waves that propagate at appropriate angles with respect to the input laser beam. But in the circumstance under discussion, phase matching can also be achieved for axial PFWM. That is, since the $4p$-$3s$ oscillator strength is small, phase-matched PFWM can also occur at UV energies that are just above the $4p_{3/2}$ and $4p_{1/2}$ levels. The medium is negatively dispersive for the UV component and phase matching can occur for exactly parallel propagation of the parametric waves (zero cone angle) [33] at frequencies where the negative dispersion of the UV light matches that of the pump laser. Except for the small frequency offset, the IR components of these axial waves appear to be due to an assumed SHR process, where in reality the SHR emission is only in the backward direction. We hasten to note that at very small detuning from the $4d$ states (small δ_2) where excitation of the $4D$ levels occurs, two additional IR lines are produced by incoherent amplified spontaneous emission (ASE) from the $4d$ state to the $4p_{3/2}$ and $4p_{1/2}$ levels. Thus at near zero detuning, six IR emissions can be resolved in the forward direction, none of which originates in a SHR process. Four forward-directed UV beams are produced (the UV emissions associated with ASE are trapped through strong absorption and are not readily detected except at intensities where self-induced transparency is produced). In the backward direction two $\sim$2.3-μm SHR emissions are produced at frequencies slightly different from any of the forward light, but no UV. (At $\delta_2 \simeq 0.0$ backward ASE is also produced, but it merges with SHR at zero detuning.)

In Fig. 7(a) we show the axial component of the IR emission associated with the $4D_{5/2} \rightarrow 4P_{3/2}$ pathway

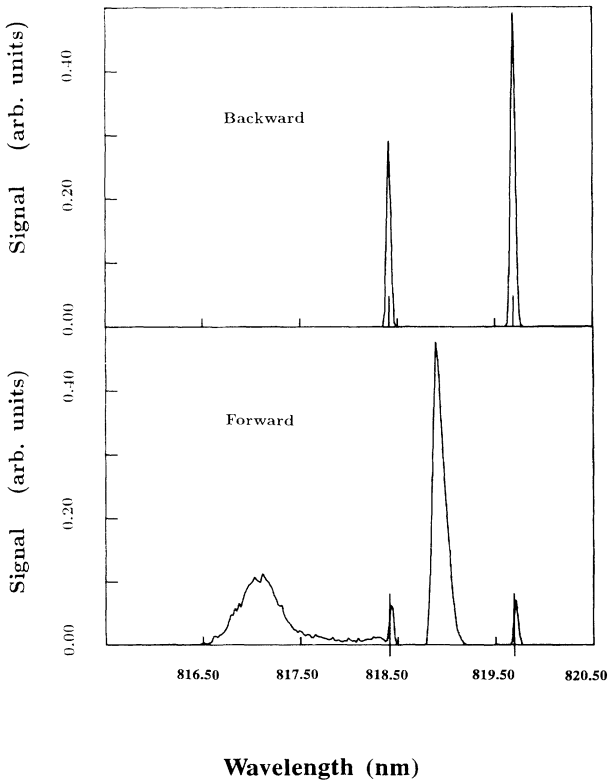

FIG. 3. Top trace: Spectral scan of backward IR emission with laser tuned to exact two-photon resonance ($\delta_2 = 0.0$). Bottom trace: Corresponding forward emission profile. $P_{Na} = 1.9$ Torr, $I_L = 8.5 \times 10^7$ W/cm^2.

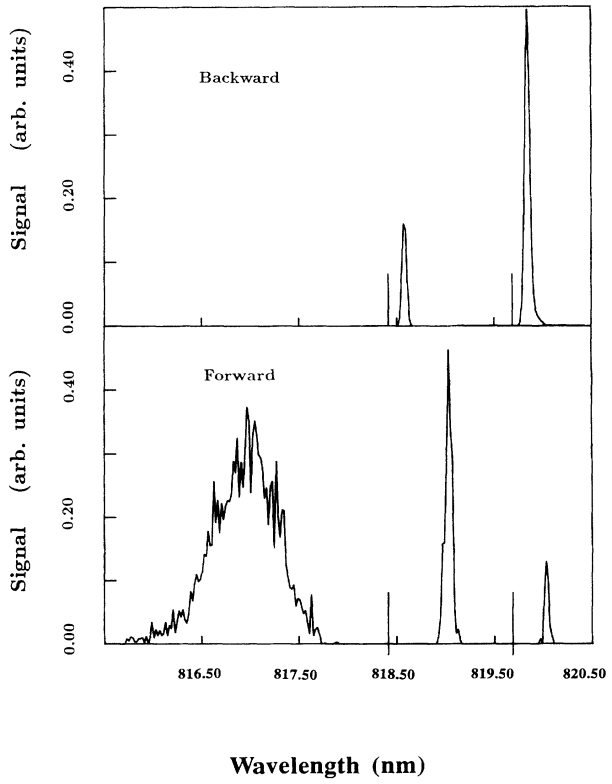

FIG. 4. Traces as in Fig. 3 but for laser detuned by 0.05 nm to long-wavelength side of two-photon resonance ($\delta_2 = 3$ cm^{-1}).

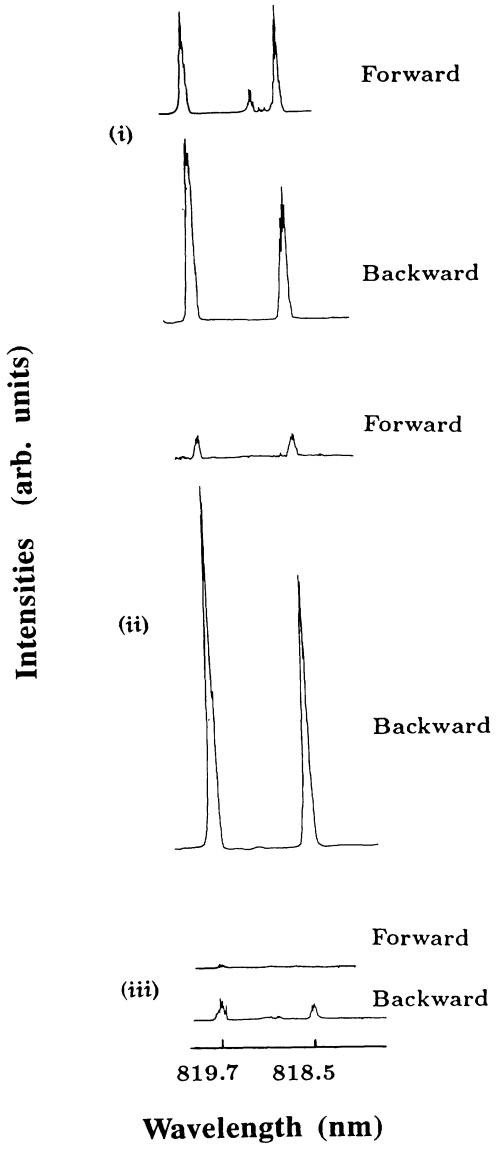

FIG. 5. Backward and forward axial emissions associated with $3D_{5/2} \rightarrow 3P_{3/2}$ and $3D_{3/2} \rightarrow 3P_{1/2}$ pathways taken at three different detunings (but with equal collection and counting efficiencies). (i) zero detuning, $\delta_2 = 0.0$; (ii) $\delta_2 = -0.01$ nm; (iii) $\delta_2 = -0.03$ nm, where δ_2 is the laser detuning from two-photon resonance. Na pressure of 2.0 Torr with 1.4 mJ/pulse laser energy.

when pumping with 9 mJ at 0.03 nm detuning from the $4D$. The upper trace shows a spectrometer scan of the backward plus forward emission, while the lower trace shows the spectral content of the backward emission. In the former, the forward PFWM component has been reflected back through the heat pipe, whereby it is clearly resolved from the SHR component.

As already noted, since the backward and forward emissions are produced by different mechanisms, the excitation profiles can look very different. In Fig. 7(b) we

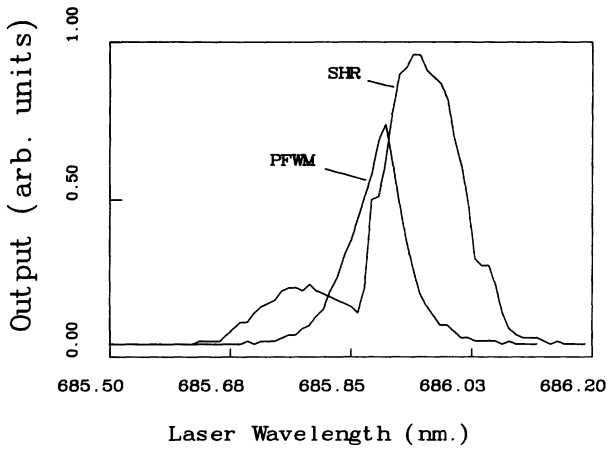

FIG. 6. Excitation profiles for forward and backward $\simeq 820$-nm emission at $P_{Na} = 1.9$ Torr and $I_L = 8.5 \times 10^7$ W/cm^2 [backward (SHR) amplitude scaled upward by factor of 3.5].

show the profiles of the forward PFWM emissions near 330 nm and the backward SHR emission near 2.3 μm as functions of laser detuning. Obviously the excitation profiles are quite different. The large dip in the SHR profile near two-photon resonance and the widths of the excitation profiles will be discussed in Sec. IV below.

C. Other metal-vapor studies

In light of the behavior of the electronic SHR scattering demonstrated here and in companion studies [19,27] it is necessary to call attention to earlier studies of SHR scattering in various metal vapors, some of which are in contradiction to the rather general feature of the process that has been presented here. That is, observations of SHR scattering have been reported where measurements were made in the forward direction. If the atomic excitations involved were also dipole coupled to the ground state, then, under conditions reported in the experiments, such emissions should have been suppressed.

The first observation of "two-photon–induced stimulated electronic Raman scattering," or SHR scattering in the present notation, was observed by Vrehen and Hikspoors [34] in Cs vapor. These authors *stated* that SHR scattering should go forward and backward, but they actually made measurements of *backward* SHR scattering to the $6p_{3/2}$ state. Since this state is dipole coupled to the ground state, the forward SHR beam should have been suppressed if they had looked for that component.

On the other hand, Cotter *et al.* [35] studied emissions near 2.3 μm from Na vapor when pumping with *circularly* polarized light near two-photon resonance with the $4d$ state at 10 Torr Na pressure. Measurements made in the forward direction were attributed to SHR emission associated with excitation of the $4p_{3/2}$ level. We note that these authors saw only one line in the IR, the component involving the $4P_{3/2}$ level, and very little UV that would correspond to ω_4 in a PFWM process. Since they used

circularly polarized pumping, this suggests that the special case, described above, for an uncanceled forward SHR was observed. However, we have conducted new experiments that contradict this interpretation, as described below.

In a detailed study of two-photon resonant PFWM in Na, Hartig [36] operated a heat pipe at 2-Torr Na pressure and recorded forward-directed emissions near 2.33 μm and 330 nm with sufficient resolution to see five of the expected $\sim$2.3-μm peaks in the IR and all four of the expected PFWM emissions near 330 nm. He did not identify all of the IR emissions, and identified only two of the UV emissions as parametric in origin, but it is evident that he actually observed two conically-phase-matched and the two axially-phase-matched PFWM processes that are expected to occur. (Hartig identified two of the UV peaks as ASE, but we observe that the UV beams are not produced in the backward direction and are thus not ASE.)

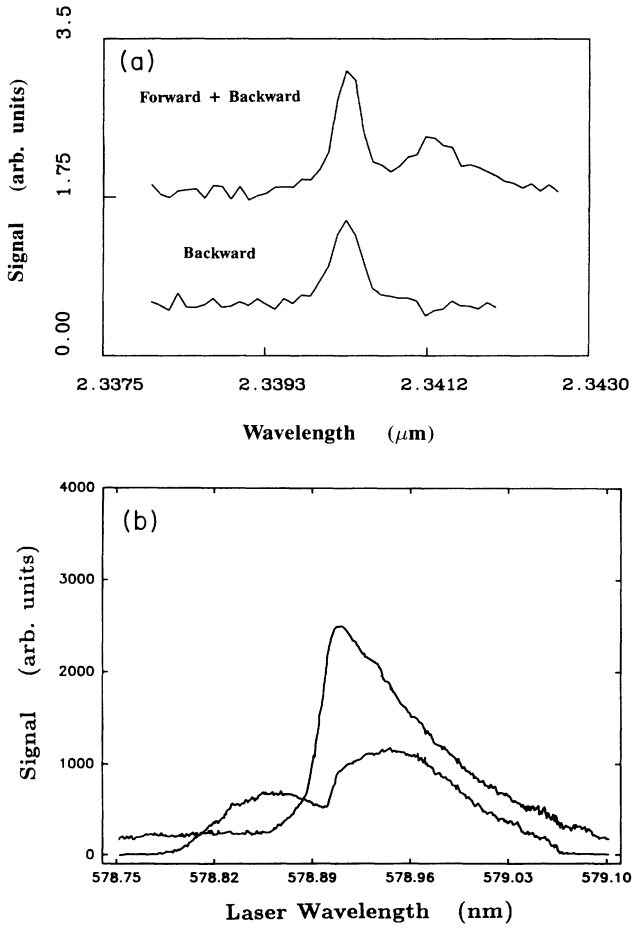

FIG. 7. (a) Spectral scans of backward (bottom) and backward plus forward (top) infrared components from SHR and FWM involving the $4P_{3/2}$ level. Na pressure 2 Torr; $E_L=9$ mJ/pulse. (b) Relative intensities of backward SHR and UV component of forward PFWM as a function of pump-laser wavelength. $P_{Na}=2.0$ Torr; pump energy$=3.5$ mJ/pulse.

A very recent study by Mori *et al.* [38] of atomic and dimer emissions from near $4d$ pumping in Na again identified forward-propagating 2.3-μm axially propagating PFWM light as SHR emission. In our previous study of this PFWM process [33], we have made the point that the emissions associated with $4d$ pumping in Na are not easy to sort out at all pressures, all pumping intensities, and all detunings, for reasons to be discussed later in this study.

Also, we note that Reif and Walther [39] studied $\simeq$16-μm photon generation in Sr vapor by two-photon pumping slightly above the $5s5d$ state with 576 nm laser photons. The tunable forward-directed 16-μm beam was attributed to SHR emission involving excitation of the $5s6p$ state. From present considerations the forward component of this SHR emission should be canceled. We suggest that the observed emission was in fact PFWM. The strontium vapor is positively dispersive at the input laser frequency. Thus PFWM can occur only for positively dispersive ω_4 ($\cong\omega_{6p\rightarrow 6s}$) and the PFWM will be axial. Since the $6p\rightarrow 6s$ oscillator strength is again very small, the phase-matching point for axial PFWM is only slightly below the $5s6p$ state, thus appearing to be SHR emission. Apparently the signature UV wave (ω_4) complementary to the 16 μm emission was not searched for, but should have been present.

We note parenthetically that in a recent paper, Krökel, Ludewigt, and Welling [40] studied frequency up-conversion in Li vapor by two-photon resonantly enhanced SHR scattering. These authors tuned near $3d$ and near $4d$ states in Li and monitored backward SHR emissions involving $2p$ excitations. In this case there was no ambiguity in the identification of the up-conversion process as SHR scattering.

Finally, we return to the observations of Cotter *et al.* [35]. In order to ascertain whether forward SHR could be produced in an experiment similar to that reported, we produced circularly polarized light near 578.8 nm with a variable retardation plate, and pumped near two-photon resonance with the $4D$ state at Na pressures from 2 to 11 Torr in focused and unfocused geometries (Lumonics HD300 dye laser, $\simeq$7 mJ/pulse, 30-cm lens). Forward and backward IR emissions near 820 nm were spectrally recorded. In the study of Ref. [35], only one emission "line" was seen in the forward IR, and no UV that corresponded to ω_4 for a PFWM process that phase matched near the $4P_{3/2}$ or $4P_{1/2}$ level was observed. Contrary to this observation, we saw forward IR emission coupled through both the $4P_{3/2}$ and the $4P_{1/2}$ sublevels, though the 3/2 component was as much as ten times brighter than that near the 1/2 level. Also we saw bright UV emission associated with the IR, only in the forward direction (easily seen, e.g., by filtering out the laser beam with a UV-transmitting filter, and observing the visible fluorescence on a white card). Thus axial PFWM was clearly and unmistakenly produced at all pressures, from 2 to 11 Torr Na pressure. The backward emission showed both components of the SHR associated with excitation of the $4P_{3/2}$ and $4P_{1/2}$ levels. But again unexpectedly, spectral resolution of the backward and forward

IR generated under all conditions of laser intensity and Na density revealed that the forward emission did not contain a SHR component for $4P_{3/2}$ excitation, even though the process should not be gain suppressed by the three-photon interference. Indeed, the behavior with circularly polarized pumping differed from that with linearly polarized pumping only in the relative efficiencies for processes associated with the 3/2 and 1/2 sublevels. The 1/2 component of the PFWM emission was much weaker under circularly polarized pumping.

On the basis of the present investigation we infer that the weak UV and single IR forward-directed beams observed by Cotter *et al.* [35] were produced by the strongest axial PFWM process. This removes the puzzle over the large widths for the IR emission profile observed in the study, since the process was not actually SHR scattering. At elevated number densities, the UV produced by PFWM becomes much weaker due to subsequent absorption [37]. But to have been unobservable, pressures would have to have been greater than the reported 10 Torr.

We have no explanation for the absence of an uncanceled forward SHR component under circularly polarized pumping. A more thorough search for this predicted behavior was made by conducting a similar experiment when tuning near-two-photon resonance with the $3D$ state in Na. This experiment also produced a negative result. Observations were similar to those with linear polarization of the pump. No SHR was observable in the forward emissions.

D. Forward suppression of five-photon hyper-Raman emission by six-wave-mixing interference

As was mentioned above, the interference effect associated with odd-photon pumping of dipole-allowed transitions is a rather general phenomenon that can become operative for any odd number of photons. Garrett, Henderson, and Payne [9] showed that direct five-photon excitation of $J=1$ levels in Xe exhibited the predicted interference. That is, the five-photon transitions were suppressed under single laser beam pumping, but were clearly evident under counterpropagating beam excitation. If we consider the five-photon extension of the hyper-Raman process we can make a prediction about the behavior of a process such as that shown in Fig. 8(a). In five-photon hyper-Raman emission, two laser photons are absorbed and three photons ω_3, ω_4, and ω_{HR} (or ω'_{HR}) are emitted, accompanied by an atomic excitation. The formalism discussed above is readily extended to yield the reduced polarization for a six-wave-mixing field at frequency $\omega_m \equiv \omega_6 = 2\omega_L - \omega_3 - \omega_4 - \omega_{HR}$. The consequences are identical to the three-photon case, namely, an interference occurs in the production of forward-directed five-photon SHR emission, due to the six-wave-mixing field associated with the forward-propagating emission. Thus we again predict that a strong asymmetry should exist between forward and backward axial emissions at ω_{HR} and ω'_{HR} in Na [Fig. 8(a)].

We have conducted experiments identical to those described above to measure forward and backward axial emissions at ω_{HR} and ω'_{HR} corresponding to five-photon excitation of $3p_{3/2}$ and $3p_{1/2}$ states, respectively, along the $4D$-$4P$-$3P$ branch. Results of these measurements are shown in Figs. 8(b) and 8(c). The data are for 3-Torr Na with 2.1 mJ/pulse pump energy at detuning $\delta_2 = -0.01$ nm. In the bottom trace the expected backward-directed five-photon SHR emissions are observed at 819.4 and 818.4 nm. In the top trace, where forward axial emission profiles are recorded, outputs at the SHR wavelengths are

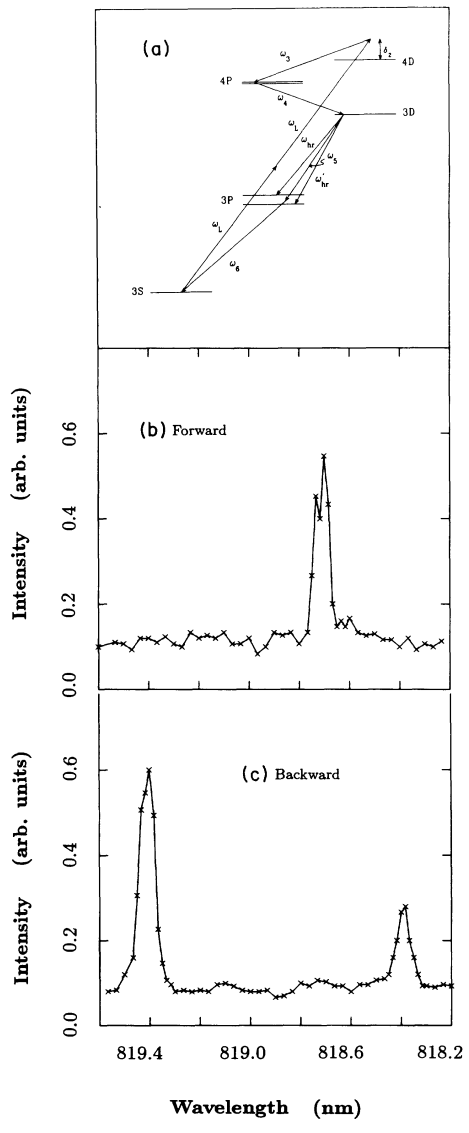

FIG. 8. Five-photon SHR process associated with excitation near the Na $4d$ state. (a) Energy-level scheme depicting the higher-order SHR process and a six-wave-mixing process proceeding along the $4d$-$4p$-$3d$-$3p$ pathway. (b) Forward axial emission. The SHR process is absent, but an axially-phase-matched six-wave-mixing process is present, as indicated in the diagram above. (c) Backward-directed five-photon SHR emissions associated with excition of $3p_{1/2}$ and $3p_{3/2}$ fine-structure levels.

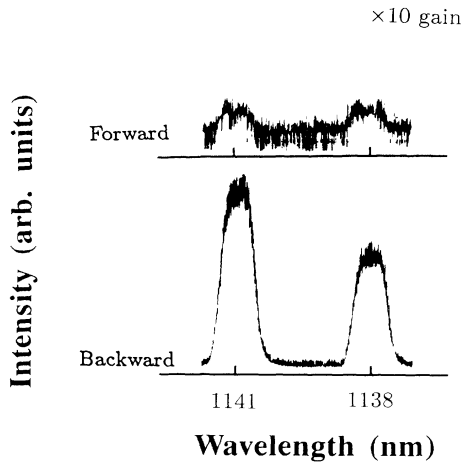

FIG. 9. Forward and backward emissions associated with excitation of the $3p_{1/2}$ and $3p_{3/2}$ fine-structure levels through a five-photon SHR process along the $4D$-$4P$-$4S$-$3P$ pathway. As in Fig. 8, the forward SHR emission is suppressed, leaving only a small $4s$-$3p$ pure ASE component in the forward direction. $P_{Na}=1.5$ Torr, $E_L=4.5$ mJ/pulse pump energy, $\delta_2=0.01$ nm.

missing. A single axial parametric six-wave-mixing process is observed in the forward direction at the expected frequency for axially-phase-matched production of ω_6 (this process is discussed in Ref. [33]). In Fig. 9 we show results from a similar scan of the emissions associated with the other branch along the $4D$-$4P$-$4S$ pathway. Here emissions near 1.1 μm are recorded in forward and backward directions. Again strong suppression of the forward versus backward emission is observed. Note that the situation is not as clean in the five-photon process, since ASE from the $3D$ (or $4S$) levels is always possible here, and it indeed goes in both directions. However, we are able to see very effective suppression of the forward gain for these higher-order odd-photon Raman-type emissions, in complete agreement with the present theoretical considerations.

IV. SATURATION BEHAVIOR IN ASE AND BACKWARD SHR DUE TO AC STARK SHIFTING BY INTERNALLY GENERATED FIELDS

From rather simple experimental measurements it is easy to establish that two-photon pumping rates for $3s\rightarrow 4d$ transitions in Na can become much reduced in an extended vapor at pressures above a fraction of a Torr, as compared to the rate produced in an atomic beam under identical pumping conditions. For example, since two-photon resonance with the $4d$ state involves photons that are only $\simeq 300$ cm^{-1} from resonance with the intermediate $3p$ state, the two-photon Rabi frequency $\Omega^{(2)}_{3s,4d}$ can easily be estimated to be $\Omega^{(2)}_{3s,4d}\simeq 500 I_p$, where the pump-laser intensity I_p is in W/cm^2. The two-photon transition rate $R_{0,2}$ at exact two-photon resonance is $R_{0,2}\simeq|\Omega^{(2)}_{0,2}|^2/\Gamma_L=1.2\times10^{-5}I_p^2$ s^{-1}, where the present laser bandwidth is $\Gamma_L=1.6\times10^{10}$ s^{-1}. Thus, for example, if $I_p=10^7$ W/cm^2, the two-photon transition to the $4d$ state is strongly saturated. In the 20-cm vapor column of the present study, the observed absorption of the unfocused pump beam at zero detuning from $4d$ resonance should be $\simeq 70\%$ for Na densities $\simeq 0.2$ Torr. (The final products from pump absorption include ionized atoms, excited atoms plus other photons, and pure photon conversion through parametric processes.) Instead, we find only about 15–20% absorption of the pump beam at 0.2 Torr Na pressure and $\simeq 25\%$ at 2.0 Torr. Thus we conclude that some mechanism is surely operative in laser propagation through an extended two-photon-resonant Na vapor medium to reduce the two-photon excitation rate from the value applicable to isolated atoms under the same laser field.

In this section we consider processes generated at and near two-photon resonance with $3D$ and $4D$ states. We describe some consequences of ac Stark shifting on the excitation rates, where the Stark effects are not produced by the laser field but by internally generated fields. We use experimental and theoretical evidence to distinguish between saturation behavior based on ac Stark-shift effects and behavior based on the coherent two-photon-resonant interference effect [20–26]. In the next section, we examine an additional saturation effect due to the coherent interference phenomenon, and attempt to outline the regimes under which these suppression mechanisms operate and/or dominate the atomic response.

Shown in Fig. 10 are the results of experimental measurements of laser beam attenuation on traversing a 20-cm Na vapor column. The laser was tuned through two-photon resonance with the $3d$ state in Fig. 10 (upper), with 0.75 mJ/pulse at Na pressure of 2.5 Torr. In Fig. 10 (lower) the laser was tuned through two-photon resonance with the $4d$ state, with 1.9 mJ/pulse at 2.5-Torr Na pressure. In the experiments, the laser beam was split 50-50 such that counterpropagating beams could traverse the Na vapor. The transmission of one beam was monitored from a small amount of light leaking through a dielectric mirror. The counterpropagating component could be blocked, so that transmission of one beam could be monitored in the presence or absence of a counterpropagating component of equal intensity, frequency, etc.

Note first that the laser beam absorption is small at $3d$ and $4d$ resonance. We find values in the range 15–25%. This same behavior was observed over a pressure range from less than 0.1 Torr up to 3 Torr. As already mentioned, in the absence of any suppression effect, the expected depletion under the conditions of the experiments would be up to 70% or more. Since the two-photon-resonant interference effect, involving PFWM fields coupling the $4D_{3/2,5/2}$ or $3D_{3/2,5/2}$ states back to the ground state, should be operative under the conditions being described, a first-order question is whether this mechanism is responsible for the diminution in beam absorption that is evident in the present data. If this is indeed the case, then as originally demonstrated by Jackson and Wynne [6], and subsequently shown in more general circumstances [7], the use of counterpropagating beams will

restore the two-photon pumping in that part of the total excitation process where one photon from each beam is absorbed. (The original demonstration by Jackson and Wynne of spoiling of the interference process through counterpropagating beams involved a three-photon process, but their same argument applies to the two-photon-resonant interference process, where one-third of the excitations in the present instance would not be canceled.) This is a consequence of the fact that no interfering PFWM field is generated through the portion of two-photon pumping in which one photon is absorbed from each oppositely directed beam. Thus on the basis of theoretical and experimental evidence, we know that if an interference effect is responsible for suppressing resonant two-photon absorption, then a large increase in the excitation rate and a corresponding increase in beam attenuation should occur when two-photon pumping is available through counterpropagating (CP) beams. In the lower traces of the upper and lower pairs in Fig. 10 we show absorption profiles in the two cases where a CP beam is spacially and temporally overlapped with the beam of which the absorption was monitored. Note that this only produces a very small increase in resonant two-photon absorption. Thus we can conclude that the two-photon excitation rate is still suppressed even when an excitation channel involving no PFWM is available. Therefore the dominant suppression mechanism is not provided by a coherent interference effect involving PFWM.

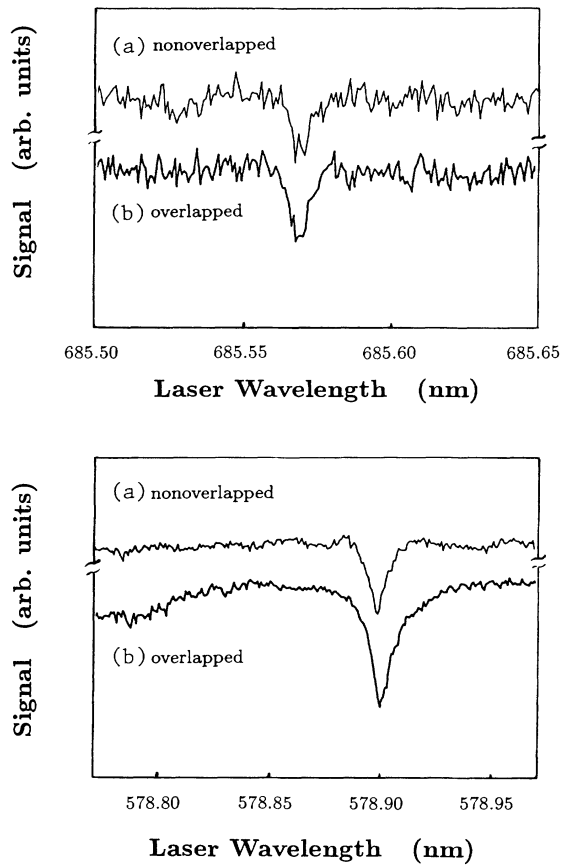

FIG. 10. Pump beam absorption profiles for tuning across two-photon resonance with $3D$ (top pair) and $4D$ (bottom pair). In both sets, the upper traces, labeled (a), show absorption of a unidirectional beam (zero suppressed) and and the lower traces, labeled (b), show the resultant absorptions for a geometry in which the pump beam is reflected and overlapped spacially and temporally with the incident pulse.

Having established through the above argument and through data such as that in Fig. 10 that the primary source of the enhanced "transparency" of the Na medium against two-photon $s \rightarrow d$ resonant absorption at $4d$ is not a PFWM interference effect, we examine any other influence that the internally generated fields might have on resonant two-photon pumping of the $s \rightarrow d$ transitions. In this regard we note, e.g., that when tuned to the $4D$ resonance at 0.2-Torr Na pressure, 2.33-μm emission associated with backward ASE to excite $4P_{1/2}$ and $4P_{3/2}$ states yields $\simeq 10^5$ W/cm^2 power densities in the infrared. This power density at 2.3 μm yields a Rabi frequency of 2×10^{11} s^{-1} between the states $|2\rangle$ and $|3\rangle$ (in this case $4d$ and $4p$ states). This corresponds to a power-broadened width of $\simeq 2$ cm^{-1}. Since the laser bandwidth is only $\simeq 0.08$ cm^{-1} full width at half maximum (FWHM) it is obvious that ac Stark shifting due to ASE or SHR photons of the observed intensity could have a dramatic influence on near-resonant two-photon excitation of the $4d$ state. The Stark shifts produced by the IR photons would be large enough to move the $4d$ level off resonance by several laser bandwidths. Thus on the bases of observed ASE or SHR outputs and estimates of the resultant one-photon Rabi frequencies, one can conclude that the effects of ac Stark shifts from the internally generated fields should be given careful attention in dealing with nonlinear effects associated with two-photon resonances.

In this section we present the results of a number of experimental observations of excitation profiles, pressure dependencies, and laser intensity dependencies of backward SHR emissions produced by tuning strong laser sources near two-photon resonance with $3d$ and $4d$ states in Na. We are able to match the observed behavior through theoretical calculations in which ac Stark effects produced by ASE or SHR fields play a dominant role in modifying the total atomic response from that predicted from elementary considerations. The details of our theoretical determinations are described in a companion paper (Ref. [27]). However, we have already noted that the magnitudes of ac Stark shifts produced by the SHR fields can be many laser bandwidths in magnitude (a few cm^{-1}) and much larger than shifts produced by the laser field itself. These shifts can cause dramatic reduction in the SHR gain, where the exact magnitude of the predicted effect depends on the model used to describe a broadband laser source. The problem has been treated for a chaotic laser field model with Lorentzian line shape, for a near continuum of longitudinal modes with random phases and a Gaussian profile for the mode intensity distribution, and in a model in which the laser is described by a multimode model in which fluctuating amplitudes and phases are randomly varied in a numerical integration of the Bloch equations in a simple three-state atomic model [27]. We simply note here that the simplified ana-

lytic model for a Gaussian laser line shape yields a reduction factor R for the SHR gain which, for $|\delta_2| \gg \Gamma_L$, and a constant hyper-Raman field [over a time $1/(4\Gamma_L)$], takes the form

$$R = \exp[-|\Omega_{2,3}^{-}(z,t)|^4/8\delta_2^2\Gamma_L^2] \ . \tag{9}$$

Here $\Omega_{2,3}^{-}(z,t)$ is the Rabi frequency between levels $|2\rangle$ and $|3\rangle$ due to the backward SHR field, δ_2 is the detuning from $|2\rangle$, and Γ_L is the laser bandwidth (where it is assumed that $|\Omega_{2,3}^{-}| \ll |\delta_2|$ and $|\delta_2| \gg \Gamma_L$ such that the amplitude of $|2\rangle$ is always small).

Alternatively the probability of excitation of state $|3\rangle$ by SHR scattering can be determined at fixed I_L and δ_2 for increasing Rabi frequency Ω_{23}^{-} between states $|2\rangle$ and $|3\rangle$. In Fig. 11 we show an example of a theoretical calculation of the transition probability for exciting state $|3\rangle$ as a function of the SHR field strength [27]. In this example the laser intensity is chosen to be 3.5×10^6 W/cm^2 at a detuning of $\delta_2=0.20$ cm^{-1}. In the figure, the solid line represents results from an approximate analytical treatment of the problem, and the points result from numerical solutions, both described in Ref. [27]. Note that the transition probability first increases with $\tau\Omega_{2,3}$ (where τ is the laser pulse length), but as the field strength continues to increase, the probability reaches a maximum, then begins to decrease rapidly for large values of $\tau\Omega_{2,3}$. Note that the suppression of the transition probability, or of the SHR gain, can indeed become very large.

To get a physical feel for the basis for the behavior exhibited in Fig. 11, we note with reference to Fig. 1 that SHR photons couple states $|2\rangle$ and $|3\rangle$ very effectively, and produce Stark shifts of both states simultaneously. The reduction of SHR gain from the ac Stark shifts arises from two mechanisms that are easily pictured but somewhat complicated to describe analytically. First, as already mentioned, the SHR-field-induced displacement of $|2\rangle$ reduces the two-photon pumping rate by producing an additional detuning of the laser field from two-photon resonance. Additionally, level $|3\rangle$ is shifted by an equal amount (the exact value varies spacially and temporally), which kills SHR gain by virtue of the required Raman frequency for exciting $|3\rangle$, having been shifted from its start-up value. The latter effect actually plays the dominant role in SHR suppression. Indeed, the region in the curve where saturation begins corresponds to values of the SHR field that produce ac Stark shifts for level $|3\rangle$, which exceed the laser bandwidth.

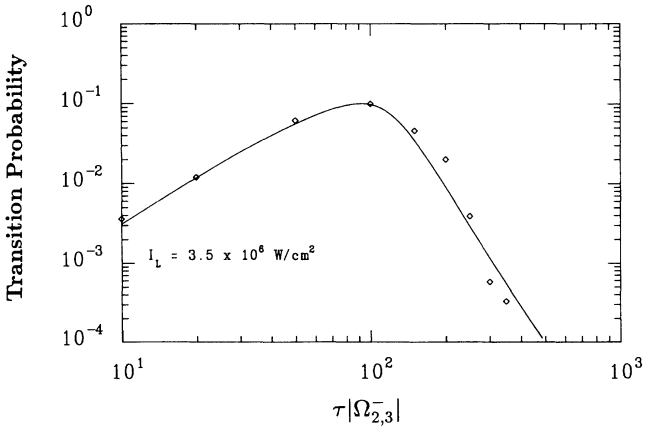

FIG. 11. Example from model calculations of the transition probability for exciting $|3\rangle$ when the pump intensity and the detuning are fixed while the SHR field strength is increased. ($I_L=3.5\times10^6$ W/cm^2 and $\delta_2=0.2$ cm^{-1}). Discrete points are results from numerical solutions with a simulated broadband laser field. Solid line from an analytic model for broadband laser excitation (see text).

The suppression of SHR gain produced by the Stark shifting becomes more and more pronounced as $|\delta_2|$ is reduced. Thus the shape of the SHR excitation profile is also strongly influenced by the ac Stark shifts. At zero detuning from two-photon resonance, where SHR goes over to ASE, the shifts are maximally effective. (The actual gain length is shortest.) This results in a distinct dip in the predicted SHR excitation profile as $|\delta_2|\rightarrow0$. For fixed laser power an increase in number density increases the total SHR emission, but the loss in gain near resonance is larger relative to that at larger detuning; thus the dip becomes more pronounced at higher number density. Examples of theoretical SHR excitation profiles are shown in Fig. 12, where the physical parameters are analogous to those for Na $4d$ resonances. The dip at $\delta_2=0$ is obviously more pronounced at higher $P_{\rm Na}$. This behavior is observed in experimental SHR excitation profiles when tuning through two-photon resonance with Na $4d$ and $3d$ states. In addition to the profile shown in Fig. 7(b) above, additional data are shown in the composite traces in Fig. 13. These data show total SHR emission associated with excitation of the $3P$ levels when tuning from -10 to $+10$ cm^{-1} across two-photon resonance with the $3D$ state at 60 MW/cm^2 laser intensity. The traces show SHR profiles at three Na pressures: 4.0, 1.4, and 0.13 Torr. Indeed, the suppression grows more pronounced at higher Na density, as predicted. The peak at $\delta_2=0.0$ is actually ASE instead of SHR emission. It too is suppressed, though the possible time delay associated with ASE changes the picture enough to modify the profile from that predicted in Fig. 12. We hasten to add that beam absorption or self-focusing effects are small enough to be discounted as possible sources of the observed behavior, whereas the calculated influence of the internally generated fields provides qualitative agreement with the experimental results for excitation profiles, and more quantitative agreement for absolute intensities, gain widths, and pressure dependencies, as described below.

In addition to a strong dip near $\delta_2=0$, the excitation profiles of the SHR emissions also show an asymmetry about the exact two-photon-resonance position at higher number densities, as can be seen in the data in Fig. 13 and in that shown in Fig. 7(b). The SHR gain tends to be lower on the high-energy side of $\delta_2=0.0$ than at a corresponding detuning on the low-energy side. Interestingly, we attribute this asymmetric gain profile to ac Stark effects also, but in this instance to a more complicated combination consisting of ac Stark shifts produced by the SHR fields combined with the shifts produced by the

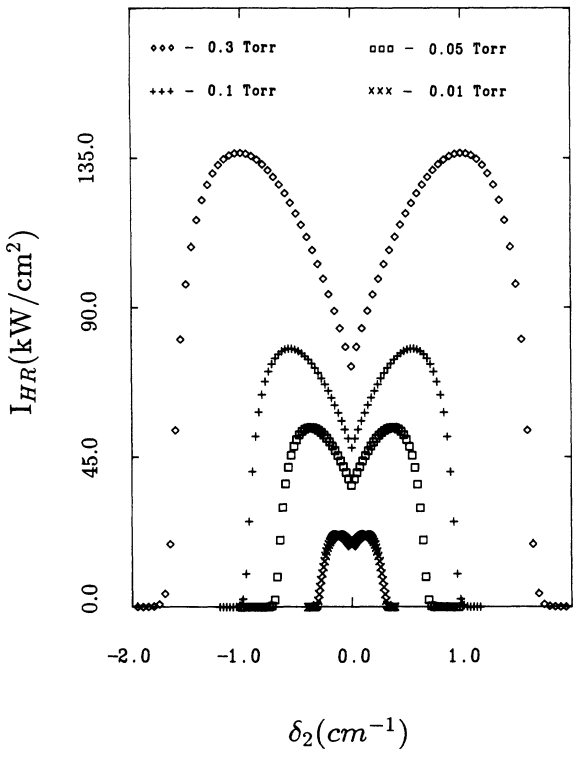

FIG. 12. Calculated intensity of SHR produced at detuning δ_2 from two-photon resonance at four different number densities. Laser bandwidth is 0.08 cm^{-1} and $I_L = 1.4 \times 10^7$ W/cm^2.

laser field. Since this asymmetry, which has also been observed by others, has not been discussed in any general sense, we note the qualitative features in more detail. For this purpose we refer to Fig. 14.

In a greatly simplified manner, the schemes depicted in Fig. 14 illustrate the directions and relative magnitudes of ac Stark shifts produced when pumping near the $3D$ and $4D$ levels of Na. In the upper pair of drawings we represent the shifts that result when tuning above (left) and below (right) the $3D$ state, i.e., positive and negative δ_2, respectively. (For simplicity the fine-structure sublevels are not shown separately.) In the lower pair we depict the behavior for tuning above and below the $4D$ state. The shifts produced by the SHR fields are shown by the dotted line extensions on the left sides of the levels. The shifts produced by the laser fields are shown on the right sides of the levels (not to exact scale). Of course the arrows should start and end on the shifted rather than on the unshifted positions, but the total shifts are the sums of the parts that we want to show separately; thus we have chosen the format depicted in the figure.

First consider the atomic response to fields associated with tuning near the $3D$ state (upper pair in Fig. 14). For this case the laser photons are $\simeq 3000$ cm^{-1} negatively detuned from the $3S \rightarrow 3P$ resonant energy and positively detuned from the $3P \rightarrow 3D$ transition. For the present discussion we choose a laser intensity of $I_L = 60.0$ MW/cm^2 (linearly polarized). The Rabi frequency for

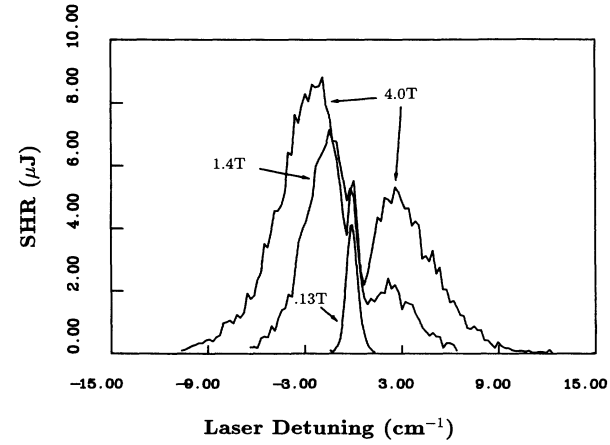

FIG. 13. Experimental excitation profiles for backward SHR emission at Na pressures of 4.0, 1.4, and 0.13 Torr as indicated. Laser intensity of 60 MW/cm^2 scanned over detuning from -15 to $+15$ cm^{-1} from two-photon resonance with the $3D$ state. (Total hyper-Raman emission near 810 nm summed over both lines.)

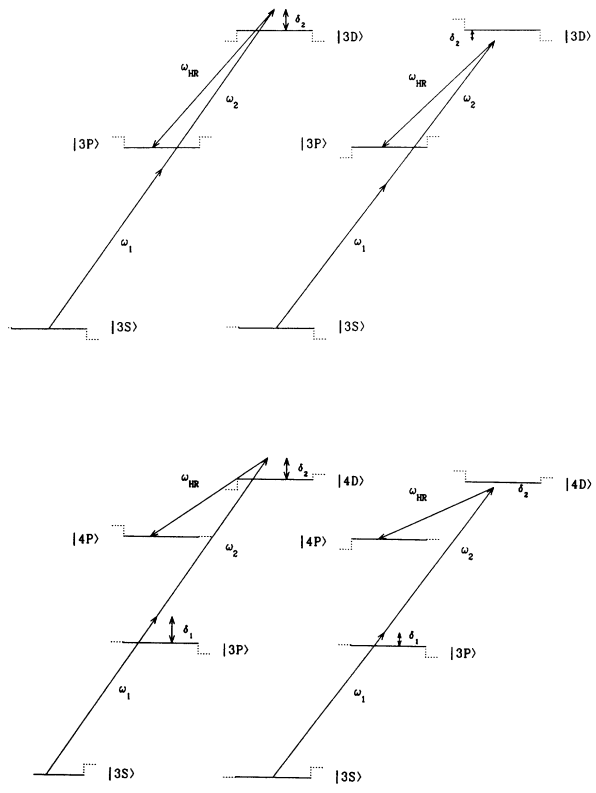

FIG. 14. Representation of ac Stark shifts associated with SHR production (not to scale). Upper pair of drawings depict level shifting for pumping above (left) and below (right) the $3D$ state. (For simplicity the fine-structure components are not shown separately.) We have chosen to show the ac Stark shifts produced by the SHR field on the left of each level while the shifts produced by the laser field are shown on the right sides. The lower pair of drawings show the same effects for tuning near the $4D$ level.

the $3S_{1/2}$-$3P_{3/2}$ component, e.g., is $\Omega_{01}=2.6\times10^8\,[I_L(\mathrm{W/cm^2})]^{1/2}$. The contribution to the ac Stark shift $\Delta_s=|\Omega_{01}|^2/\delta_1$ is 0.08 $\mathrm{cm^{-1}}$. The ground state is moved downward and the $3P_{3/2}$ upward. (The $3P_{1/2}$ is moved upward by half this amount and the ground-state downward shift is added to by a similar contribution.) The corresponding Rabi frequency for the upper $3P_{3/2}$-$3D_{5/2}$ transition is $\Omega_{12}=1.07\times10^8\,[I_L(W/\mathrm{cm^2})]^{1/2}$. Since $\delta_2\ll\delta_1$ the detuning is again 3000 $\mathrm{cm^{-1}}$, but positive. The shift for 60 $\mathrm{MW/cm^2}$ is 0.16 $\mathrm{cm^{-1}}$ upward for the $3P$ and downward for the $3D$.

Next consider the SHR field associated with $3P$ excitation, which we choose in this example to have an intensity $I_{\mathrm{HR}}=2.4\times10^4$ $\mathrm{W/cm^2}$ ($\simeq4$ μJ in Fig. 13). Since δ_2 is small, the SHR field is quite effective in producing shifts in $3P$ and $3D$ levels. The signs of the level shifts now depend on whether the laser is tuned above or below $3D$. For $\delta_2=2$ $\mathrm{cm^{-1}}$, in this example, $\Delta_s=0.42$ $\mathrm{cm^{-1}}$. For positive δ_2 level $|2\rangle$ is moved down and $|3\rangle$ is moved upward, and vice versa for negative detuning (Fig. 13). (The effect of the SHR field on $|0\rangle$ is negligible.)

Now for this example we examine the effects of the various shifts on SHR gain. Note that the shifts of $|2\rangle$ and $|3\rangle$ from the SHR field are the largest in magnitude of all shift components. Recall also in this context that a shift in $|3\rangle$ due to a build up in the SHR intensity leads to a much more effective suppression of SHR gain than does a shift of the same magnitude in $|2\rangle$. The two-photon-resonant enhancement is reduced by a shift-induced increase in the magnitude of δ_2, independent of whether the sign of δ_2 is positive or negative. The gain $g_{\mathrm{SHR}}\propto(\delta_2)^{-2}$. On the other hand, a shift in the position of $|3\rangle$ affects the SHR gain by reducing the gain length. Once the intensity of the backward beam builds up to a point where the SHR-induced shift exceeds the laser bandwidth, the gain for HR photons that started up from noise at a frequency corresponding to the unshifted level position falls to zero. The gain length is thereby foreshortened, since the SHR must start up again at a frequency corresponding to the shifted position. This effect, if considered alone, results in a large overall reduction in the SHR gain [27], which is symmetric in δ_2. The combined effects of the SHR-induced shifting of $|2\rangle$ and $|3\rangle$ on total SHR output was depicted in Fig. 12.

Now consider the shifts induced by the *laser field.* (The effect of ac Stark shifts from the laser field on stimulated Raman emission, as opposed to SHR emission, has been treated recently by Kryzhanovsky *et al.* [41]. They considered stimulated Raman production associated with tuning near an upper one-photon resonance in Ba.) Here the laser-induced shifts are not altered in magnitude or sign as δ_2 is scanned over a small range near two-photon resonance, but the effect that laser-induced shifts can have on SHR gain is complicated by the fact that the laser and the SHR fields propagate in opposite directions. Qualitatively, when the laser is detuned above the $3D$ state, the shift of the $3P$ level from the laser field and from the SHR field is in the same direction. The gain reduction is magnified by the sum of the shifts. However, when the laser is tuned on the low-energy side of the $3D$, the shifts of the $3p$ from these fields are in opposite directions. The gain reduction caused by the SHR shift is now reduced by the partially offsetting shift due to the laser field. Moreover, the shifts of the $3D$ level from the two fields also add for blue-side detuning and subtract for red-side pumping. Thus the gain reduction due to modification of δ_2 is also greater for blue-side as opposed to red-side detuning. The result is that a rather larger asymmetry in the gain for SHR production is evident with much higher output for a given detuning below the $3D$ than for an identical magnitude detuning above the $3D$. This is the behavior exhibited in Fig. 13 and other excitation profiles observed in SHR associated with pumping near the $3D$.

Now consider briefly the situation for tuning around the $4D$ two-photon resonance. Here the laser field (which was typically only $\simeq10^7$ $\mathrm{W/cm^2}$) produces only a small shift in the final state, i.e., the $4P$. Thus it adds or subtracts very little to or from the large shifts produced by the SHR field on the $4P$ level. The shift of the $4D$ levels from this laser intensity is also small ($\simeq0.1$ $\mathrm{cm^{-1}}$). However, the shift of the ground state is not so small ($\simeq-1$ $\mathrm{cm^{-1}}$ in this example). With reference to the bottom pair of diagrams in Fig. 13 we see that this shift reduces the magnitude of δ_2 for red-side detuning and increases it for blue-side detuning. The effect is again similar to the $3D$ case in that the SHR gain is enhanced on one side and reduced on the other side of two-photon resonance, though the effect is less pronounced in the case of the $4D$ as compared to the $3D$. Indeed, the data shown in Fig. 7(b) above and in Fig. 13 of Ref. [25] show an asymmetry in the SHR excitation profile that is enhanced at red- versus blue-side laser settings, but that is less pronounced than for the corresponding $3D$ profiles.

Finally we consider three other consequences of ac Stark shifting on SHR emissions. We note comparisons of predicted and experimental forms of the laser-power dependence of the SHR production, the full width at half maximum of the SHR profile, and the intensity of the SHR as functions of Na number density.

Figure 15 shows the energy of backward SHR emission versus laser intensity for laser pumping at a detuning of 0.01 nm below the $4d$ state, at 0.07 Torr Na. On the basis of the theoretical model discussed elsewhere [27], in which the combined shifting of $|2\rangle$ (here the $4d$ state) and of $|3\rangle$ (here either of the $3p$ levels) suppresses the SHR emission, we predict that the form of I_{HR} should change with increasing I_L from a dependence based on I_L^2 gain over to a form in which I_{HR} is almost a linear function of I_L. As can be seen in Fig. 15, the SHR energy becomes almost exactly linear (within experimental error) with laser energy for all values above a critical value—here 0.06 mJ/pulse. Thus this feature agrees well with our theoretical model.

In Fig. 16 we show the width of the SHR excitation profile as a function of P_{Na}. The data were taken at a maximum laser intensity of 2.2×10^7 $\mathrm{W/cm^2}$ at beam center. The SHR profile is rather irregular in shape due to the strong influence of Stark suppression on SHR gain. However, at sufficiently large detuning, where the gain is

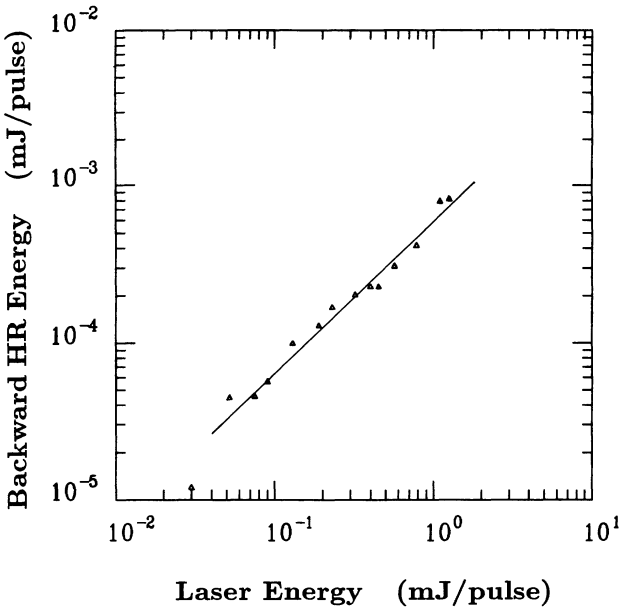

FIG. 15. Energy per pulse, as a function of incident laser intensity, of backward stimulated hyper-Raman emission associated with pumping near the $4D$ states. ($\lambda_{HR} \simeq 2.3$ μm.) $P_{Na} = 0.07$ Torr. The solid line is a curve of slope = 1.0.

not suppressed by the shifts, we note the simple fact that in this region $g = AP_{Na}/\delta_2^2$, where A is a constant. But when the gain reaches a sufficiently large magnitude, it becomes limited by the shifting mechanism, changing very rapidly at smaller detuning to a value smaller than that predicted by the A/δ_2^2 form. Thus one can define an effective width W for the SHR excitation profile as that extending to a value of δ_2, where the gain reaches the limiting value. Here we choose this as the position where g yields 32 e folds in the SHR field. That is, at $\delta_2 = (AP_{Na}/g)^{1/2}$, we have a width relationship

$$W = 2\delta_2 = \sqrt{A/g}\,\sqrt{P_{Na}}\ .$$

At fixed laser power, the SHR profile will have an irregular shape due to the Stark-related suppression near $\delta_2 = 0$, but it should have a "width" that is proportional to $\sqrt{P_{Na}}$. This predicted form agrees well with the data shown in Fig. 15. The solid line is the predicted form. The agreement between theory and experiment extends over two orders of magnitude in P_{Na}.

Finally, in Fig. 17 we show the strength of the SHR signal as a function of P_{Na}, under the same laser power as that of Fig. 16. The predictions of SHR signal strength as a function of P_{Na} are more complicated. Numerical studies yield a form again close to $\sqrt{P_{Na}}$, but not quite. The predicted form is that shown in the solid line. Details of the calculation are given in another paper [27]. The agreement between theoretically and experimentally determined SHR intensities, though not as close as the widths, is still rather good.

We note parenthetically that the production of self-limiting ac Stark shifting by the SHR process will produce another feature in the SHR emission, which we will call pulse smoothing. With relatively broadband multimode lasers, such as those used in the present study, an individual pulse contains a number of amplitude fluctuations in which the intensity changes greatly on a picosecond time scale. Any nonlinear process, such as SHR or FWM, will ordinarily have the highest gain during peak power intervals within a pulse. However, when an intensity peak builds up in the SHR field, the ac Stark shift that results from this field lowers the gain in this portion of a pulse as compared to that in somewhat lower intensity portions of the pulse. This results in an amplitude leveling of the backward-propagating SHR field. This effect has not been verified in the present set of experiments.

In concluding this section we reiterate that strong suppression effects are operative in SHR emission in an

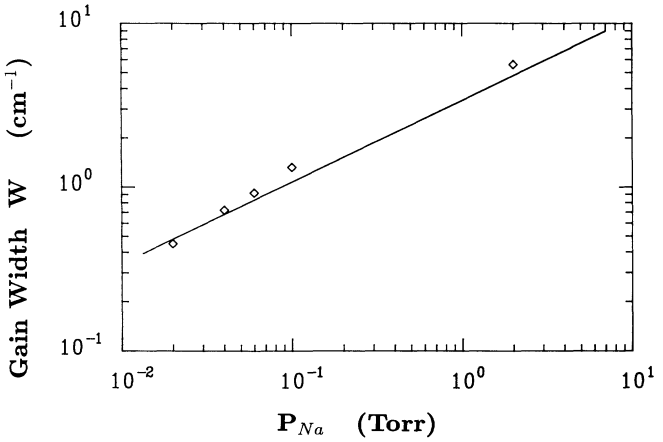

FIG. 16. Effective width of the stimulated hyper-Raman emission profile as a function of Na pressure. Laser power density is 2.2×10^7 W/cm^2 at beam center. Solid line is the theoretically predicted $[(P_{Na})^{1/2})]$ form.

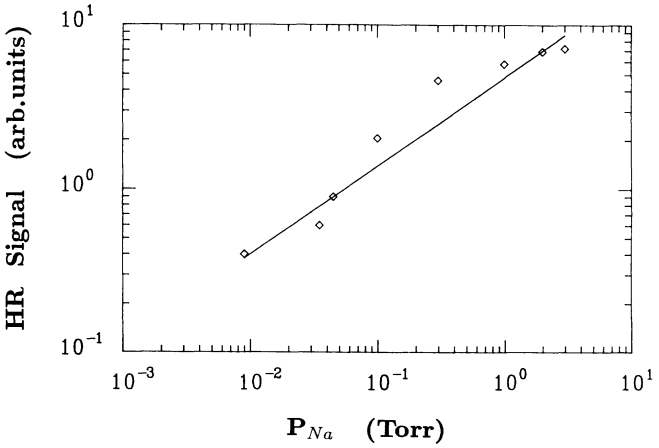

FIG. 17. Intensity of the SHR emission as a function of Na pressure for fixed input laser power. Solid line is the predicted $[(P_{Na})^{1/2}]$ form.

extended nonlinear medium, and that much of the backward SHR behavior is dominated by ac Stark-shifting mechanisms. Observations of several of the features of SHR emissions in Na vapor and in Xe are in fairly good agreement with predictions.

V. SATURATION OF PARAMETRIC FOUR-WAVE MIXING DUE TO TWO-PHOTON INTERFERENCE EFFECT

We have presented evidence that a major source of suppression of resonant two-photon excitations of Na $4d$ states is due to Stark shifting rather than to an interference effect involving PFWM. On the other hand, the even-parity interference effect involving PFWM can be produced under the circumstances of this study. As already mentioned in the Introduction, recent experimental studies by Malcuit, Gauthier, and Boyd [21] and by Krasnikov, Pshenichnikov, and Solomatin [22] demonstrated a suppression of resonant two-photon excitation probabilities for $s \rightarrow d$ and $s \rightarrow s$ transitions, respectively, in dense sodium vapor. In an early theoretical study of resonant two-photon absorption processes, Manykin and Afanas'ev [20] predicted that two-photon absorption could be reduced if different laser beams were used to drive a given two-photon transition by two different routes, satisfying $\Delta k = 0$ between the two pathways. Subsequently, the theory was extended [20] to show that the population of a resonantly pumped two-photon state could be reduced to zero under circumstances where a second laser, tuned near a one-photon allowed state, produced four-wave mixing, again with the restriction that $\Delta k = 0$ for the FWM process. The latter process is that which was demonstrated in Ref. [22], where resonant two-photon $3s \rightarrow 4s$ transitions in Na vapor were observed to be reduced in the presence of FWM driven by a third laser beam (described as "parametric brightening"). Other density-dependent features of the same process were reported more recently by the same authors [42]. The effect of this interference process was revealed independently in the context of two-photon resonantly enhanced third harmonic production by Kildal and Brueck [43]. It was also examined recently by Smith, Alford, and Hadley [44] in studies of four-wave mixing in Hg vapor.

A detailed examination of the influence of the two-photon interference in pumping near Na $4D$ states has been given recently by the present authors [25,26,33]. Here we present some additional features of the effects of this phenomenon on PFWM and we discuss the predictions and observations associated with this third type of suppression mechanism in order to put it into some perspective with respect to the two processes discussed above. In the studies under discussion, all three mechanisms become operative under circumstances that can be fairly reliably predicted.

In the even-parity interference process, two-photon pumping from the ground state, $|0\rangle$, to a two-photon level, $|2\rangle$, by laser photons ω_1 and ω_2 with reduced two-photon Rabi frequency $\Omega_{02}^{(2)}$ produces two new frequencies ω_3 and ω_4 through PFWM. These generated fields create a second two-photon rate $\tilde{\Omega}_{02}^{(2)}$ between the same two states. Under phase-matched PFWM generation, the second pathway destructively interferes with the first [1,2,6,7], that is, in the equations of motion, the two-photon pumping rate by the laser field, $\Omega_{02}^{(2)}$, is cancelled by the two-photon rate $\tilde{\Omega}_{02}^{(2)}$ due to PFWM. The two rates become equal in magnitude and opposite in sign. Under these conditions the "effective" two-photon Rabi rate between $|0\rangle$ and $|2\rangle$ goes to zero. Since photons generated through PFWM are almost resonant with intermediate p states, the two Rabi rates can become equal in magnitude even though the fields involved in $\tilde{\Omega}_{02}^{(2)}$ are fairly weak as compared to the laser field. Manykin and Afanas'ev [6] showed that solutions to the equations of motion with $\Delta k = 0$ always evolve to the destructive interfering phase relationship at zero detuning from two-photon resonance. Experimental studies of the interference associated with resonant two-photon pumping in Na vapors have so far involved some way of monitoring the influence of PFWM on the resonant transfer of population to the two-photon-resonant state [1–4]. However, the interference effect also has a strong and easily demonstrated influence on PFWM intensities that are produced when tuning near two-photon resonances. We describe here some of the experimental and theoretical consequences of this effect.

If we ignore the fine-structure splittings in Na, we can describe the PFWM problem by a four-level system, as depicted in the leftmost branch of Fig. 1. (In the present context we label ω_3 as ω_{IR} and ω_4 as ω_{UV}. The process differs from SHR by the presence of the detuning δ_3 from state $|3\rangle$.) We choose a simpler phase convention than that of Eq. (1) and assume the time-dependent state vector of an atom at z to be of the form

$$|\Psi(z,t)\rangle = \sum_{n=0}^{3} a_n(z,t) e^{-i\omega_n t} |n\rangle \ . \tag{10}$$

The fields are written as

$$E_3(z,t) \equiv E_{\mathrm{IR}}(z,t) = \tfrac{1}{2} E_{\mathrm{IR}}^{(0)} e^{i(\omega_{\mathrm{IR}} t - k_{\mathrm{IR}} z)} + \mathrm{c.c.} \ , \tag{11a}$$

$$E_4(z,t) \equiv E_{\mathrm{UV}}(z,t) = \tfrac{1}{2} E_{\mathrm{UV}}^{(0)} e^{-i(\omega_{\mathrm{UV}} t - k_{\mathrm{UV}} z)} + \mathrm{c.c.} \ , \tag{11b}$$

and the corresponding reduced Rabi frequencies are defined as

$$\Omega_{23}(z,t) = D_{2,3} E_{\mathrm{IR}} / 2\hbar \ , \tag{12a}$$

$$\Omega_{30}(z,t) = D_{3,0} E_{\mathrm{UV}} / 2\hbar \ . \tag{12b}$$

A perturbation treatment in the rotating-wave approximation yields equations for the a_n's of the form

$$\dot{a}_0(z,t)=i\Omega_{02}^{(2)}e^{i\delta_2 t}e^{-i2k_L z}a_2(z,t)+i\Omega_{03}e^{i\delta_3 t}e^{ik_{UV}z}a_3(z,t)\ ,$$
$$\dot{a}_2(z,t)=i\Omega_{20}^{(2)}e^{-i\delta_2 t}e^{i2k_L z}a_0(z,t)+i\Omega_{23}e^{-i(\omega_{IR}-\omega_{23})t}e^{ik_{IR}z}a_3(z,t)\ , \tag{13}$$
$$\dot{a}_3(z,t)=i\Omega_{30}e^{i\delta_3 t}e^{ik_{UV}z}a_0(z,t)+i\Omega_{32}e^{i(\omega_{IR}-\omega_{23})t}e^{-ik_{IR}z}a_2(z,t)\ ,$$

where $2\Omega_{23}$ is the actual Rabi frequency between $|2\rangle$ and $|3\rangle$, etc. The intermediate state $|1\rangle$ (here the $3P$ state of Na) was adiabatically eliminated, thereby reducing the problem to a three-level system with an effective two-photon coupling expressed through the two-photon Rabi frequency $2\Omega_{02}^{(2)}$ between $|0\rangle$ and $|2\rangle$,

$$\Omega_{02}^{(2)}=\Omega_{01}\Omega_{12}/\delta_1\ . \tag{14}$$

Equations (13) are solved to third order for the a_n's under conditions of low population transfer, i.e., $a_0\simeq 1$. Under these conditions the solutions to (13) are

$$a_0(z,t)\approx 1\ ,$$
$$a_2(z,t)=-\frac{e^{-i\delta_2 t}}{\delta_2}\left[\Omega_{20}^{(2)}e^{i2k_L z}-\frac{\Omega_{23}\Omega_{30}}{\delta_3}e^{i(k_{IR}+k_{UV})z}\right], \tag{15}$$
$$a_3(z,t)=-\frac{e^{-i\delta_3 t}}{\delta_3}\left[\Omega_{30}e^{ik_{UV}z}-\frac{\Omega_{32}\Omega_{20}^{(2)}}{\delta_2}e^{i(2k_L-k_{IR})z}+\frac{\Omega_{30}|\Omega_{23}|^2}{\delta_2\delta_3}e^{ik_{UV}z}\right].$$

From these solutions one can also write the nonlinear polarization source terms for the PFWM waves at frequencies ω_3 and ω_4. Thus

$$P^{NL}(\omega_3)=ND_{3,2}\langle\langle a_2 a_3^*\rangle\rangle e^{-i(\omega_2-\omega_3)t}+\text{c.c.} \tag{16}$$

A similar expression involving $(a_3 a_0^*)$ is obtained for $P^{NL}(\omega_4)$. The results are

$$P^{NL}(\omega_3)\equiv P^{NL}(\omega_{IR})=ND_{2,3}\frac{e^{-i(\omega_{IR}t-k_{IR}z)}}{\Delta_2\delta_3}\left[\Omega_{20}^{(2)}\Omega_{03}e^{-i\Delta kz}-\frac{1}{\delta_3}\Omega_{23}|\Omega_{03}|^2\right]+\text{c.c.}\ , \tag{17}$$

$$P^{NL}(\omega_4)\equiv P^{NL}(\omega_{UV})=ND_{0,3}\frac{e^{-i(\omega_{UV}t-k_{UV}z)}}{\Delta_2\delta_3}\left[\Omega_{20}^{(2)}\Omega_{32}e^{-i\Delta kz}-\frac{1}{\delta_3}\Omega_{30}|\Omega_{23}|^2\right]+\text{c.c.} \tag{18}$$

Here $\Delta_2=\delta_2+\Gamma$, where Γ allows for collisional dephasing and laser bandwidth effects.

To obtain equations for the field generated at ω_3 and ω_4, Maxwell's equation is solved in the slowly varying envelope approximation with the nonlinear polarizations as source terms. The equations for $E_{IR}\equiv E_3(\omega_3)$ and $E_{UV}\equiv E_4(\omega_4)$, expressed in terms of the Rabi frequencies, are

$$\frac{d\Omega_{23}}{dz}=N\frac{2i\pi\omega_{IR}}{\hbar cn(\omega_{IR})}\frac{|D_{2,3}|^2}{\Delta_2\delta_3}\left[\Omega_{20}^{(2)}\Omega_{03}e^{-i\Delta kz}-\frac{1}{\delta_3}\Omega_{23}|\Omega_{03}|^2\right], \tag{19a}$$

$$\frac{d\Omega_{30}}{dz}=N\frac{2i\pi\omega_{UV}}{\hbar cn(\omega_{UV})}\frac{|D_{0,3}|^2}{\Delta_2\delta_3}\left[\Omega_{20}^{(2)}\Omega_{32}e^{-i\Delta kz}-\frac{1}{\delta_3}\Omega_{30}|\Omega_{23}|^2\right]$$
$$=N\frac{2i\pi\omega_{UV}}{\hbar cn(\omega_{UV})}\frac{|D_{0,3}|^2}{\Delta_2\delta_3}e^{-i\Delta kz}\Omega_{32}\times\left[\Omega_{20}^{(2)}-e^{i\Delta kz}\frac{1}{\delta_3}\Omega_{30}\Omega_{23}\right], \tag{19b}$$

or

$$\frac{d\Omega_{23}}{dz}=N\frac{2i\pi\omega_{IR}}{\hbar cn(\omega_{IR})}\frac{|D_{2,3}|^2}{\Delta_2\delta_3}e^{-i\Delta kz}\Omega_{03}\Omega_{\text{eff}}^{(2)}\ , \tag{20a}$$

$$\frac{d\Omega_{30}}{dz}=N\frac{2i\pi\omega_{UV}}{\hbar cn(\omega_{UV})}\frac{|D_{0,3}|^2}{\Delta_2\delta_3}e^{-i\Delta kz}\Omega_{32}\Omega_{\text{eff}}^{(2)}\ . \tag{20b}$$

The effective two-photon Rabi frequency $\Omega_{\text{eff}}^{(2)}$ is, in the notation of the introduction to this section, $\Omega_{\text{eff}}^{(2)}=\Omega_{20}^{(2)}+\tilde{\Omega}_{20}^{(2)}$, where $\tilde{\Omega}_{02}^{(2)}=-\Omega_{23}\Omega_{30}e^{i\Delta kz}/\delta_3$. From the results of Manykin and Afanas'ev we know that the phase-matched solutions evolve such that $\tilde{\Omega}_{02}^{(2)}=-\Omega_{02}^{(2)}$; that is,

$$\Omega_{23}\Omega_{30}/\delta_3\rightarrow\Omega_{01}\Omega_{12}/\delta_1\ . \tag{21}$$

The fields only grow appreciably when $\Delta k\rightarrow 0$, where the phase mismatch Δk is given by $\Delta k=k_{UV}+k_{IR}-2k_L$. Under these circumstances the effective two-photon Rabi frequency $\Omega_{\text{eff}}^{(2)}=(\Omega_{20}^{(2)}-\Omega_{23}\Omega_{30}e^{i\Delta kz}/\delta_3)\rightarrow 0$ when $\Delta k=0$. That is, the two-photon Rabi frequency is cancelled out by destructive interference from the phase-matched PFWM. This causes the nonlinear polarizations at ω_{IR} and ω_{UV} and the PFWM gain to go to zero at a critical depth into the nonlinear medium, at the point where $\tilde{\Omega}_{02}^{(2)}$ grows to be equal in magnitude to $\Omega_{02}^{(2)}$. At this point, additional propagation through the medium produces no

additional growth in the generated fields. Alternatively, for fixed laser-power density, the PFWM production in a given column length will grow with number density until $\Omega_{\text{eff}}^{(2)}$ vanishes within the length of the medium. A further increase in number density will not increase PFWM output. The point at which the interference grows in simply moves toward the entrance end of the medium as the number density is increased.

This particular influence of the interference effect on PFWM is clearly demonstrated in the data shown in Fig. 18. Illustrated is the total output of the $\simeq$330-nm component of PFWM produced in tuning 0.03 nm from two-photon resonance with the Na $4D$ state with 34 MW/cm^2 laser power density. Note that output as a function of Na number density saturates at $P_{\text{Na}} \simeq 0.4$ Torr. A further increase in Na pressure produces no additional PFWM output, in agreement with the predicted interference behavior. The complementary wave at ω_{IR} behaves in exactly the same manner (see Fig. 10 of Ref. [41]).

We note that there are actually four frequency components of the $\simeq$330-nm emission. Two of these are phase matched through emission at a small angle about the laser beam at frequencies that are positively dispersive for ω_4 (i.e., for frequencies that correspond to phase-matching points slightly below the energy of the $4P_{3/2}$ level and another slightly below the $4P_{1/2}$ level). Two other components are produced through axial-phase-matched PFWM, which occurs at frequencies that are negatively dispersive at ω_4. One of these points lies at about 2 cm^{-1} above the $4P_{3/2}$ level and another at $\simeq 1$ cm^{-1} above the $4P_{1/2}$ level. The characteristics of the phase-matching conditions for PFWM near the Na $4P$ levels are extensively discussed elsewhere by the present authors [33]. Discussed also is the fact that the conical PFWM associated with pathways through the $3P_{3/2}$ and $3P_{1/2}$ fine-structure levels is much weaker and can be neglected in the context of the interference behavior. We simply note that the axially-phase-matched components strongly dominate the PFWM process, which greatly simplifies analysis of the interference problem. The PFWM intensity plotted in Fig. 18 is the sum of the ω_{UV} components from each of the axially-phase-matched processes.

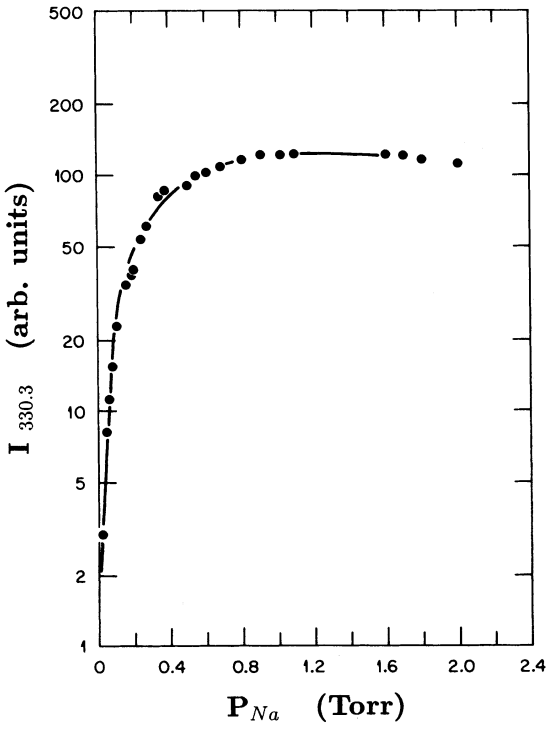

FIG. 18. Output of the UV components (ω_{UV}) of the axial PFWM process as a function of Na pressure at a fixed laser frequency. Laser detuning was 0.03 nm on the high-energy side of the $4d$ resonance. $I_P = 34.0$ MW/cm^2.

The interference effect has several other consequences for PFWM production under circumstances where the conditions for the interference at the two-photon level are satisfied. From Eqs. (20a) and (20b) it is easy to show that the generated fields E_{IR} and E_{UV} at frequencies ω_{IR} and ω_{UV} obey a constant of motion [25] such that

$$\frac{E_{\text{IR}}^2}{\omega_{\text{IR}}} - \frac{E_{\text{UV}}^2}{\omega_{\text{UV}}} = \text{const} . \tag{22}$$

That is, the change in photon number at ω_{IR} is equal to the change at ω_{UV}. Therefore, under conditions where neither of the generated fields is preferentially absorbed, we can write $I_{\text{IR}} = I_{\text{UV}}(\omega_{\text{IR}}/\omega_{\text{UV}})$. That is, the intensity at ω_{IR} is proportional to that at ω_{UV}. But when the fields grow to the point where Eq. (21) becomes satisfied, we have the added condition that

$$I_{\text{IR}}^{1/2} I_{\text{UV}}^{1/2} = C I_L^{1/2} I_L^{1/2} ,$$

where $C = \delta_3 D_{0,1} D_{1,2} / (\delta_1 D_{2,3} D_{3,0})$. Since $I_{\text{IR}} \propto I_{\text{UV}}$, this means that

$$I_{\text{IR}} \propto I_L$$

(also $I_{\text{UV}} \propto I_L$). Thus the intensity of the PFWM beams at ω_3 and ω_4 will grow *linearly* with laser pump intensity, once the interference condition is achieved. Consequently, at a given pressure, the fields at ω_{IR} or ω_{UV} would grow nonlinearly with laser intensity at low pump intensities, but linearly at laser intensities above a critical cancellation value I_c. This influence of the interference effect on PFWM output is clearly revealed in the data of Fig. 19, where we plot the total 2.33-μm IR intensity versus pump power density for two different sodium pressures. In the lower curve (0.35-Torr Na) the yield suddenly changes to a linear dependence on laser intensity I_L at a critical intensity I_c of 0.85 MW/cm^2 (laser tuned onto $4d$ resonance). For a given vapor density and column length, the critical laser intensity is that which produces PFWM of intensity just sufficient to satisfy Eq. (21) at the exit end of the vapor column. At a higher P_{Na} of 2 Torr (upper curve) the onset of the interference occurs at a lower laser intensity. A longer column length would similarly give a lower I_c for a given density, again in a predictable manner. In the examples shown here the two-photon Rabi rates, which we calculate on the basis of intensities of the PFWM and laser fields, the detunings,

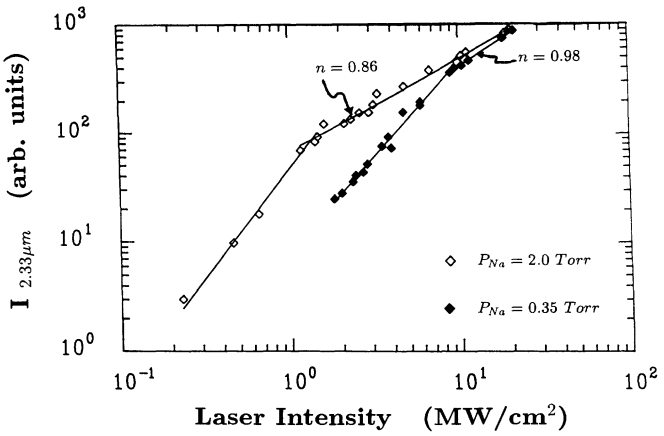

FIG. 19. Intensity of forward axial 2.33-μm PFWM emission $I_{2.33\ \mu m}$ as a function of pump-laser intensity I_L at fixed pump-laser frequency ($\delta_2=0.0$). Data are for Na pressures of 2.0 and 0.35 Torr. Straight lines are computer fits to the data in separate intensity regions for each pressure. For laser intensities above a critical value I_c the power dependence for the PFWM output is predicted to go as $(I_L)^n$ where $n=1$. At 2.0 Torr Na pressure, $I_c=1.3$ MW/cm^2. At 0.35 Torr, $I_c=8.4$ MW/cm^2.

and the known oscillator strengths, satisfy the condition $\Omega^{(2)}_{0,2}=\tilde{\Omega}^{(2)}_{0,2}$ to an accuracy of 15%.

The results plotted in Fig. 19 show a fourth property of the PFWM generation under the influence of the interference effect. The gain for PFWM varies as a constant times $P_{\rm Na}I_L/(\delta_3\Delta_2)$. The critical laser intensity I_C for which the interference sets in (causing the functional form of $I_{\rm PFWM}$ to go linear in I_L) is that which produces the necessary magnitude of PFWM gain within the full length L of the vapor zone. Thus, to a good approximation, the product of critical laser intensity and sodium pressure should be a constant in experiments conducted at different Na pressures. This property holds for the data of Fig. 19, where for data taken at two different number densities, $I_cP_{\rm Na}\cong 2.7$ Torr MW/cm^2.

A fifth predicted feature of PFWM generation under the influence of the interference effect is shown in Fig. 19; namely, above the critical intensity where the outputs of the PFWM components go linear with laser intensity, the intensities should merge to a common yield curve for all Na densities. Indeed, we see from the data in the figure that total PFWM intensities at 2.0 and 0.35 Torr converge to a common curve in the laser intensity region where outputs at both densities become linear in I_L.

There is yet a sixth and rather novel result of the influence of the interference effect on four-wave mixing. Since PFWM output becomes limited when the two-photon Rabi rate from the parametric waves $\Omega^{(2)}_{\rm PFWM}$ becomes equal in magnitude to that from the laser pumping $\Omega^{(2)}_L$, then for a given $\Omega^{(2)}_L$ a PFWM process involving a large nonlinear susceptibility will, under conditions of two-photon cancellation, produce less output than one with a smaller $\chi^{(3)}$. This last predicted feature has not been demonstrated in the present set of experimental studies.

Finally we note another aspect of the PFWM behavior. The good agreement between measured and predicted features due to the two-photon interference was observed only in the case of pumping near the $4D$ level where axial FWM production dominates. The PFWM emissions produced when pumping near the $3D$, where almost all PFWM output is generated through angle phase matching, did not yield similar two-photon cancellation-effect behavior under any conditions of pressure, pump intensity, or detuning. The conical emission problem is much more difficult to describe theoretically. We have no good explanation for the marked differences in the PFWM behavior between the $3D$ and $4D$ cases. It is interesting in this regard to note that in the first experimental study of the two-photon interference effect by Boyd *et al.*, the linear dependence of the PFWM output on input laser intensity could have been extracted from their equations, but was not. Instead, they inferred that the dependence should be quadratic, and further showed a quadratic dependence of the PFWM intensity with laser energy. Thus their data actually agreed with our present observation, that the two-photon interference effect does not limit the conical PFWM emissions associated with $3D$ pumping in the way that the simple theory predicts.

VI. CONCLUSIONS

In these studies of two-photon resonantly enhanced SHR and PFWM emissions, we have attempted to verify as many as possible of the features that can occur as a result of the interplay between the pump fields and the fields generated within the nonlinear medium. In the particular case of pumping near the $4D$ state in Na, where axial emission processes are dominant, we have a fairly global picture of the total atomic response. The overall picture is rather complicated, but can be summarized and generalized as follows.

(i) At pressures high enough to observe SHR emissions in the present experiments, the SHR emissions are suppressed in the forward direction. This suppression is produced by interference from four-wave mixing for the three-photon hyper-Raman process and by a six-wave-mixing interference in the case of the five-photon hyper-Raman processes.

ac Stark effects due to the SHR fields produce several influences on SHR emission. Thus as a consequence of the Stark shifting we see, in addition, the following.

(ii) The SHR excitation profiles develop, under some conditions, a pronounced dip at exact two-photon resonance, and an asymmetry for equal detuning above and below the resonance.

(iii) The SHR output versus laser intensity goes approximately linear under strong two-photon pumping.

(iv) An effective width for the excitation profile is produced that is proportional to $(P_{\rm Na})^{1/2}$.

(v) The SHR peak amplitude versus $P_{\rm Na}$ varies as $(P_{\rm Na})^{1/2}$.

(vi) The temporal profile of SHR pulses produced by a

multimode laser pump should be drastically smoother under conditions where SHR gain is reduced by the ac Stark effect.

Finally, the effect of the two-photon interference on axial PFWM in Na has several additional consequences.

(vii) The gain for axially-phase-matched PFWM saturates with pressure above a certain critical pressure.

(viii) Alternatively, the PFWM gain saturates with column length for a given pressure of the vapor column.

(ix) The intensity of PFWM output goes linear in laser intensity above a critical intensity.

(x) The product of critical intensity times number density is a constant.

(xi) Plots of I_{PFWM} versus I_L for different number densities all merge to a common linear curve when the laser intensities exceed I_c.

(xii) If two PFWM processes were pumped with equal two-photon Rabi rates, then under conditions of cancellation at the two-photon level, one would have the seemingly contradictory result that the process with the smaller $\chi^{(3)}$ will have the higher intensity.

ACKNOWLEDGMENT

Research was sponsored by the Office of Health and Environmental Research, U.S. Department of Energy under Contract No. DE-AC05-84OR21400 with Martin Marietta Energy Systems, Inc.

*Present address: Department of Physics, Davidson College, Davidson, NC.

†Also at Department of Physics, University of Tennessee, Knoxville, TN. Present address: JILA, Boulder, CO.

[1] R. N. Compton, J. C. Miller, A. E. Carter, and P. Kruit, Chem. Phys. Lett. **71**, 87 (1980).

[2] J. C. Miller, R. N. Compton, M. G. Payne, and W. R. Garrett, Phys. Rev. Lett. **45**, 114 (1980).

[3] M. G. Payne, W. R. Garrett, and H. C. Baker, Chem. Phys. Lett. **75**, 468 (1980); M. G. Payne and W. R. Garrett, Phys. Rev. A **26**, 356 (1982).

[4] J. C. Miller and R. N. Compton, Phys. Rev. A **25**, 2056 (1982).

[5] J. H. Glownia and R. K. Sander, Appl. Phys. Lett. **49**, 21 (1982).

[6] D. J. Jackson and J. J. Wynne, Phys. Rev. Lett. **49**, 543 (1982).

[7] W. R. Garrett, W. R. Ferrell, M. G. Payne, and J. C. Miller, Phys. Rev. A **34**, 1165 (1986).

[8] W. R. Garrett, S. D. Henderson, and M. G. Payne, Phys. Rev. A **34**, 3463 (1986).

[9] W. R. Garrett, S. D. Henderson, and M. G. Payne, Phys. Rev. A **35**, 5032 (1987).

[10] M. N. R. Ashfold, C. D. Heryet, J. D. Prince, and B. Tutcher, Chem. Phys. Lett. **131**, 291 (1986).

[11] T. M. Orlando, L. Li, S. L. Anderson, and M. G. White, Chem. Phys. Lett. **129**, 31 (1986).

[12] L. Li, M. Wu, and P. M. Johnson, J. Chem. Phys. **86**, 1131 (1987).

[13] C. Chen, Y. Y. Yin, and D. S. Elliott, Phys. Rev. Lett. **64**, 57 (1990).

[14] M. G. Payne and W. R. Garrett, Phys. Rev. A **26**, 356 (1982); **28**, 3409 (1983).

[15] D. J. Jackson, J. J. Wynne, and P. H. Kes, Phys. Rev. A **28**, 781 (1983).

[16] J. J. Wynne, Phys. Rev. Lett. **52**, 751 (1984).

[17] G. S. Agarwal and S. P. Tewari, Phys. Rev. A **29**, 1922 (1984).

[18] M. G. Payne, W. R. Garrett, and W. R. Ferrell, Phys. Rev. A **34**, 1143 (1986).

[19] M. A. Moore, W. R. Garrett, and M. G. Payne, Opt. Commun. **68**, 310 (1988); W. R. Garrett, M. A. Moore, R. K. Wunderlich, and M. G. Payne, in *Resonance Ionization Spectroscopy, 1988,* edited by T. B. Lucatorto and J. E. Parks (Hilger, Bristol, 1989), p. 33.

[20] E. A. Manykin and A. M. Afanas'ev, Zh. Eskp. Teor. Fiz. **48**, 931 (1965) [Sov. Phys. JETP **21**, 619 (1965)]; *ibid.* **52**, 1246 (1967) [**25**, 828 (1967)].

[21] M. S. Malcuit, D. J. Gauthier, and R. W. Boyd, Phys. Rev. Lett. **55**, 1086 (1985); R. W. Boyd, M. S. Malcuit, D. J. Gauthier, and K. Rzazewski, Phys. Rev. A **35**, 1648 (1987).

[22] V. V. Krasnikov, M. S. Pshenichnikov, and V. S. Solomatin, Pis'ma Zh. Eksp. Teor. Fiz. **43**, 115 (1986) [JETP Lett. **43**, 148 (1986)].

[23] G. S. Agarwal, Phys. Rev. Lett. **57**, 827 (1986).

[24] R. K. Wunderlich, M. G. Payne, and W. R. Garrett, in *Resonance Ionization Spectroscopy, 1986,* edited by G. S. Hurst and C. G. Morgan (Hilger, Bristol, 1987), p. 269; S. J. Bajic, R. N. Compton, J. A. D. Stockdale, and D. D. Konowalow, J. Chem. Phys. **89**, 7056 (1988).

[25] R. K. Wunderlich, W. R. Garrett, R. C. Hart, M. A. Moore, and M. G. Payne, Phys. Rev. A **41**, 6345 (1990).

[26] W. R. Garrett, R. C. Hart, M. A. Moore, M. G. Payne, and R. K. Wunderlich, *Coherence and Quantum Optics VII,* edited by J. H. Eberly, L. Mandel, and E. Wolf (Plenum, New York, 1989), p. 389.

[27] M. G. Payne and W. R. Garrett (unpublished).

[28] W. R. Garrett, R. C. Hart, J. C. Miller, M. G. Payne, and J. E. Wray, Opt. Commun. **86**, 205 (1991).

[29] M. G. Payne and W. R. Garrett, Phys. Rev. A **42**, 1434 (1990).

[30] W. R. Garrett, R. C. Hart, J. C. Wray, I. Datskou, and M. G. Payne, Phys. Rev. Lett. **64**, 1717 (1990); M. G. Payne, W. R. Garrett, R. C. Hart, and I. Datskou, Phys. Rev. A **42**, 2756 (1990).

[31] Yu. P Malakyan, Opt. Commun. **69**, 315 (1989).

[32] J. Krasinski, D. J. Gauthier, M. S. Malcuit, and R. W. Boyd, Opt. Commun. **54**, 241 (1985).

[33] M. A. Moore, W. R. Garrett, and M. G. Payne, Phys. Rev. A **39**, 3692 (1989).

[34] Q. H. F. Vrehen and H. M. J. Hikspoors, Opt. Commun. **21**, 127 (1977).

[35] D. Cotter, D. C. Hanna, W. H. W. Tuttlebee, and M. A. Yaratich, Opt. Commun. **22**, 190 (1977).

[36] W. Hartig, Appl. Phys. **15**, 427 (1978).

[37] R. K. Wunderlich, M. A. Moore, W. R. Garrett, and M. G. Payne, in *Resonance Ionization Spectroscopy, 1988,* (Ref. [19]), p 49.

[38] K. Mori, Y. Yasuda, N. Sokabe, and A. Murai, Opt. Commun. **57**, 418 (1986).

[39] J. Reif and H. Walther, Appl. Phys. **15**, 361 (1978).

[40] D. Krökel, L. Ludewigt, and H. Welling, IEEE J. Quantum Electron. **QE-22**, 489 (1986).
[41] B. V. Kryzhanovsky, S. O. Sapondzhyan, D. G. Sarkisyan, and G. A. Torosyan, Opt. Commun. **71**, 381 (1989).
[42] V. V. Krasnikov, M. S. Pshenichnikov, and V. S. Solomatin, Kvant. Electron. (Moscow) **15**, 1587 (1988) [Sov. J. Quantum Electron. **18**, 991 (1988)].
[43] H. Kildel and S. R. Bureck, IEEE J. Quantum Electron. **QE - 16**, 566 (1980).
[44] A. V. Smith, W. J. Alford, and G. R. Hadley, J. Opt. Soc. Am. B **5**, 1503 (1988).